Materials Today Bio 17 (2022) 100441

Contents lists available at ScienceDirect

Materials Today Bio

journal homepage: www.journals.elsevier.com/materials-today-bio

Optical diagnostic imaging and therapy for thyroid cancer

Chengying Shao [a,b,1], Zhenfang Li [c,1], Chengchi Zhang [d], Wanchen Zhang [a,b], Ru He [c], Jiajie Xu [a,f,*], Yu Cai [e,**]

[a] Otolaryngology& Head and Neck Center, Cancer Center, Department of Head and Neck Surgery, Zhejiang Provincial People's Hospital (Affiliated People's Hospital, Hangzhou Medical College), Hangzhou, Zhejiang 310014, China
[b] Second Clinical Medical College, Zhejiang Chinese Medical University, Hangzhou 310053, China
[c] School of Basic Medical Sciences and Forensic Medicine, Hangzhou Medical College, Hangzhou 310012, China
[d] Zhejiang University of Technology, Hangzhou, 310023, China
[e] Clinical Research Institute, Zhejiang Provincial People's Hospital, Affiliated People's Hospital of Hangzhou Medical College, Hangzhou, China
[f] Key Laboratory of Endocrine Gland Diseases of Zhejiang Province, Hangzhou 310014, China

ARTICLE INFO

Keywords:
Optical imaging
Phototherapy
Thyroid cancer
Multimodal therapy
Optical imaging-guided surgery

ABSTRACT

Thyroid cancer, as one of the most common endocrine cancers, has seen a surge in incidence in recent years. This is most likely due to the lack of specificity and accuracy of its traditional diagnostic modalities, leading to the overdiagnosis of thyroid nodules. Although there are several treatment options available, they are limited to surgery and ^{131}I radiation therapy that come with significant side effects and hence cannot meet the treatment needs of anaplastic thyroid carcinoma with very high malignancy. Optical imaging that utilizes optical absorption, refraction and scattering properties, not only observes the structure and function of cells, tissues, organs, or even the whole organism to assist in diagnosis, but can also be used to perform optical therapy to achieve targeted non-invasive and precise treatment of thyroid cancer. These applications of screening, diagnosis, and treatment, lend to optical imaging's promising potential within the realm of thyroid cancer surgical navigation. Over the past decade, research on optical imaging in the diagnosis and treatment of thyroid cancer has been growing year by year, but no comprehensive review on this topic has been published. Here, we review key advances in the application of optical imaging in the diagnosis and treatment of thyroid cancer and discuss the challenges and potential for clinical translation of this technology.

Abbreviations: ^{131}I-BSA@CuS, ^{131}I-labeled BSA-modified CuS nanoparticles; 5-ALA, 5-Aminolevulinic acid; ASIR, age-standardized rates of cancer incidence; ATC, anaplastic thyroid carcinoma; AuNCs@BSA-I, innovative iodinated gold nanoclusters; Au@MSNs, photo-triggered Gold nanodots capped mesoporous silica nanoparticles; BRAF, V-Raf murine sarcoma viral oncogene homolog B; CBDCA, Carboplatin; CDFI, color doppler flow imaging ultrasound; ECDT, enhanced chemodynamical therapy; CLND, central compartmentalized node dissection; CPDA-^{131}I NPs, the ^{131}I-radiolabeled cerebroid polydopamine nano-particles; CT, Computed Tomography; DOT, Diffuse Optical Tomography; DTC, differentiated thyroid cancer; EGF, epidermal growth factor; EGFR, epidermal growth factor receptor; ESMO, European Society of Medical Oncology; FDA, U.S. Food and Drug Administration; FI, fluorescence imaging; FNAB, fine-needle aspiration biopsy; FNAs, fine needle aspirations; FTC, follicular thyroid carcinoma; GC, germinal center; HAOA, Hyaluronic Acid and Oleic Acid; HYP, hypericin; ICG, indocyanine green; IJV, internal jugular vein; IR825@B-PPNs, Polymeric NPs with bevacizumab and IR825 conjugated on the surface; L-A PTA, laparoscopic photothermal ablation; MDR, multidrug resistance; mETE, microscopic extrathyroidal extension; MTC, medullary thyroid carcinoma; NIR, near-infrared; NIRF, near-infrared fluorescence; NIR-FI, near-infrared fluorescence imaging; NIR-PIT, near-infrared photoimmunotherapy; NMRI, Nuclear Magnetic Resonance Imaging; OCT, Optical Coherence Tomography; OI, optical imaging; OS, overall survival; PAI, Photoacoustic Imaging; Pd-MOF, porphyrin–palladium metal–organic framework; PDT, photodynamic therapy; PET, Positron Emission Tomography; PGs, parathyroid glands; PLP, porphyrin-HDL nanoparticle; PTA, photothermal reagents; PTC, papillary thyroid carcinoma; PTT, photothermal therapy; RIT, radioactive iodine therapy; ROS, reactive oxygen species; SEC, Selenocysteine; SiRNA, interfering RNA; SV, subclavian vein; TC, thyroid cancer; TD, Thoracic Duct; TF, tissue factor.

* Corresponding author. Otolaryngology& Head and Neck Center, Cancer Center, Department of Head and Neck Surgery, Zhejiang Provincial People's Hospital (Affiliated People's Hospital, Hangzhou Medical College), Hangzhou, Zhejiang, 310014, China.
** Corresponding author.
E-mail addresses: xujiajie@hmc.edu.cn (J. Xu), caiyu@hmc.edu.cn (Y. Cai).
[1] These authors contributed equally to this work.

https://doi.org/10.1016/j.mtbio.2022.100441
Received 7 August 2022; Received in revised form 22 September 2022; Accepted 24 September 2022
Available online 26 September 2022

1. Introduction

Thyroid cancer (TC) is currently the most common endocrine cancer (Table 1) [1] and has seen a significant increase in incidence over recent decades. However, such an increase in incidence may be attributed to overdiagnosis of thyroid nodules [2–4], thus recommended therapeutic interventions for TC have become increasingly conservative [5,6]. According to guidelines of the European Society of Medical Oncology (ESMO), the main therapeutic options for differentiated thyroid cancer (DTC) include thyroidectomy, lymph node dissection, and ^{131}I therapy [7]. Additionally, radioactive iodine therapy (RIT) when used alone may be sufficient. Yet, there are also studies that suggest the incidence of TC is indeed increasing based on statistical numbers regarding advanced TC and morbidity-based mortality [8]. Papillary carcinomas (PTC, 80%), follicular carcinomas (FTC, 10%), and medullary thyroid carcinomas (MTC, 5–10%) make up the bulk of TCs. An uncommon but deadly form of TC is anaplastic thyroid carcinoma (ATC). Patients with ATC who received multimodal therapy and palliative care had median overall survival (OS) times of 21 months and 3.9 months, respectively [9].

The primary treatment for DTC is surgery, supplemented by endocrine therapy, radiotherapy and others [6,10], yielding a satisfactory prognosis overall. Of these, Transoral/transaxillary thyroidectomy has gained popularity since it addresses issues of neck scars, which is an important aspect for young and middle-aged women - a demographic at the highest risk of DTC. However, complications such as nerve injuries and accidental damage to the parathyroid glands still occur occasionally in lumpectomy procedures, and may include temporary or permanent hypoparathyroidism, injury or paralysis of the recurrent laryngeal nerve, celiac fistula, Horner's syndrome, cervical motor nerve injury, and hematoma or plasmacytoma formation [11]. Given this, more emphasis is placed on improving the quality-of-life post-surgery. To achieve this goal, surgical treatment of TC tends to minimize the invasion of surrounding normal tissues while ensuring the survival rate. What remains are the more troublesome forms of TC such as ATC, where mortality is close to 100% as a result of the absence of effective therapy. The variety, complexity, and diversity of malignant tumors are often to blame for the monotherapy modality's low effectiveness and high recurrence rate, and researchers have been exploring novel treatments for TC to overcome such challenges.

To solve the above-mentioned diagnostic and therapeutic challenges of TC, optical diagnostic imaging and phototherapy possessing great potential have entered the view of researchers. Optical imaging (OI), which has benefits such as high spatial and temporal resolution, high sensitivity, high contrast, high throughput, non-invasive, simple equipment, and low cost, uses a variety of optical properties like absorption, scattering, reflection, and fluorescence [12] to visualize specimens such as cells, tissues, organs, and even complete living creatures. OI has been also widely employed in clinical practice for other fields, such as in liver and breast cancer [13,14], gram-negative bacillary infections [15], endocrine diseases [16] and other conditions that have seen success. Additionally optical probes have even been successfully used in environmental science to detect chemical contamination [17–19]. Currently, options of OI include Fluorescence Imaging (FI), Optical Coherence Tomography (OCT), Endoscopy, Photoacoustic Imaging (PAI), Diffuse Optical Tomography (DOT), Raman Spectroscopy, and Super-resolution Microscopy. In this review, we will thoroughly summarize the progress of OI in terms of diagnosis, phototherapy, and combination therapy in TC. The main challenges and opportunities for the clinical application of OI are also discussed.

2. Optical diagnostic imaging for TC

Overdiagnosis of thyroid nodules is seen as one of the reasons for their proliferating global incidence, and could potential be addressed through OI technology. To our knowledge, u25ltrasonography relies on the image quality, neck coverage area, and interpretation by the diagnostic sonographer. Quite often many ambiguous thyroid nodules require further invasive testing - fine needle aspiration biopsy (FNAB) - to distinguish between benign and malignant nodules. Currently, the fine-needle aspiration biopsy (FNAB) is the gold standard for determining whether to pursue medical interventions for thyroid nodules. For 15–20% of overall cases termed “suspicious” or “inconclusive”, total thyroidectomy is typically selected. However, histological investigations showed that only 25–50% of cases that received thyroidectomy are malignant. OI is more effective than traditional medical imaging techniques in numerous areas, including [20]:(1) High biocompatibility and safety; (2) Wide range of imaging windows; (3) Ability to combine with other imaging modalities to create multi-dimensional diagnostic imaging; (4) Capturing high-quality images of ex vivo, in vivo, and in vitro specimens; (5) Providing data on biochemical processes, biological dynamics, and other topics; (6) High molecular specificity achieved through flexible modifiability.

2.1. Fluorescence imaging (FI)

When a fluorescent substance is irradiated by light, it will emit light of different colors and intensities, and when the irradiation stops, the emitted light will soon disappear. Exogenous fluorescent probes can be artificially designed to possess distinctive fluorescence in the ultraviolet, visible or near-infrared spectra. Their situated environment (polarity, refractive index, viscosity, etc.) can sensitively change their fluorescence properties, such as excitation wavelength, emission wavelength, lifetime, and intensity. FI is one of the essential imaging methods for enhancing bio-diagnosis and image-guided surgeries in both basic research and therapeutic applications (Scheme 1). FI provides benefits over conventional imaging methods, including X-ray Computed Tomography (CT), Nuclear Magnetic Resonance Imaging (NMRI), and Positron Emission Tomography (PET) in terms of high spatial and temporal resolution, non-invasiveness, real-time imaging, and cost efficiency. Using this highly sensitive imaging technique, it can provide a good indication of the

Table 1
Age-standardized rates of cancer incidence (ASIR) per 100,000 [1].

Rank	China			Sex	Rank	US			Sex
	Tumor location	Cases (%)	ASIR			Tumor location	Cases (%)	ASIR	
7th	Thyroid	221,093 (4.8)	11.30	Both	12th	Thyroid	52,912 (2.3)	11.80	Both
9th	Thyroid	53,389 (2.2)	5.40	Male	15th	Thyroid	14,351 (1.2)	6.10	Male
4th	Thyroid	167,704 (8.0)	17.50	Female	6th	Thyroid	38,561 (3.7)	17.40	Female
Rank	UK			Sex	Rank	Worldwide			Sex
	Tumor location	Cases (%)	ASIR			Tumor location	Cases (%)	ASIR	
19th	Thyroid	5527 (1.2)	6.10	Both	9th	Thyroid	586,202 (3.0)	6.60	Both
20th	Thyroid	1385 (0.6)	2.90	Male	16th	Thyroid	137,287 (1.4)	3.10	Male
11th	Thyroid	4142 (2.0)	9.20	Female	5th	Thyroid	448,915 (4.9)	10.10	Female

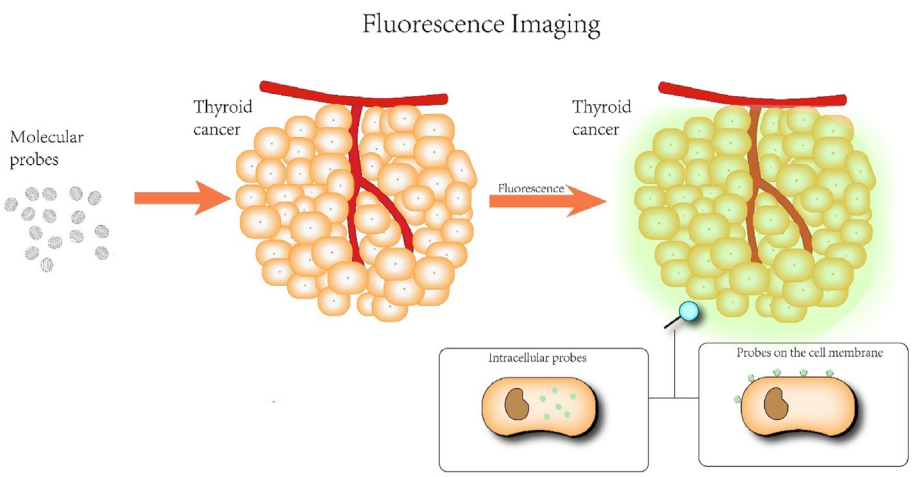

Scheme 1. Schematic diagram of fluorescence imaging.

molecular or cellular level activity, which is indispensable for our understanding of biological processes and disorders. FI has so far been widely used for immunofluorescence analysis, imaging, drug distribution and metabolism detection, and imaging-guided surgery [21].

As one of the vital components of FI, near-Infrared fluorescence imaging (NIR-FI) is a developing non-invasive imaging modality with distinct benefits in biological imaging, disease diagnosis, and surgical navigation due to its high sensitivity and instantaneous nature. The NIR windows are currently divided into NIR-I (750–900 nm) and NIR-II (1000–1700 nm) categories. A narrow absorption peak at 1400–1500 nm caused by water overtones is excluded from the NIR–II window, which is further separated into NIR–IIa (1000–1400 nm) and NIR–IIb (1500–1700 nm) [22]. According to a recent study, the NIR-II region could also be defined as 900–1880 nm, meanwhile, it creatively suggested excellent-performance imaging in 1400–1500, 1700–1880, and 2080–2340 nm wavelengths, designating them as NIR-IIx, NIR-IIc, and NIR-III, respectively [23]. Because of its capacity to penetrate deep tissues, little photon scattering, and constrained autofluorescence, NIR light in the second optical window, such as NIR-IIb, 1500–1700 nm, is well suited for imaging live creatures with great spatiotemporal resolution [24]. As a result, there has been a steady rise in the emphasis of relevant research from NIR- I imaging to NIR- II imaging.

NIR-II imaging molecular probes are clinically important for detecting tumor biomarkers with high sensitivity, monitoring tumor vasculogenesis, and predicting tumor invasiveness and prognosis. NIR-II imaging only offers a two-dimensional picture of the target when used alone for tumor identification, and the absence of fine-grained spatial information may result in erroneous target description [25]. Therefore, dual-modality or even multi-modality diagnostic imaging has become a trend. Xin Chen et al. developed innovative iodinated gold nanoclusters (AuNCs@BSA-I) probes based on dual-mode fluorescence/CT imaging for the visualization of thyroid malignancies [26]. The signal background ratio of AuNCs@BSA-I in normal thyroid tissue is "fast in, slow out," while in thyroid tumors, a partial fluorescence signal appears at 1.5 h and disappears rapidly at 2.5 h, with a signal background ratio of "slow in, fast out". AuNCs@BSA-I is a great selective nanoprobe for TC diagnosis. Meanwhile, research [27] has constructed magnetic resonance imaging/fluorescence lifetime dual-modality imaging nanoprobes-targeting two peptides (peptide1 and peptide7) of Galectin-1 conjugated with ultra-small superparamagnetic iron oxide particles (USPIO) or a NIR dye (CF770), embodying the high specificity and sensitivity for the PTC detection of 75% and 100%, respectively. In addition, one study [28] created a multimodal imaging platform called LUCA that combines clinical ultrasound, 16-channel diffuse correlation spectroscopy, and eight-wavelength near-infrared time-resolved spectroscopy in a single device to increase the specificity and sensitivity of TC diagnosis.

In an alternative to direct imaging of the thyroid gland for diagnosis, a number of biochemical metabolites can be detected to facilitate the

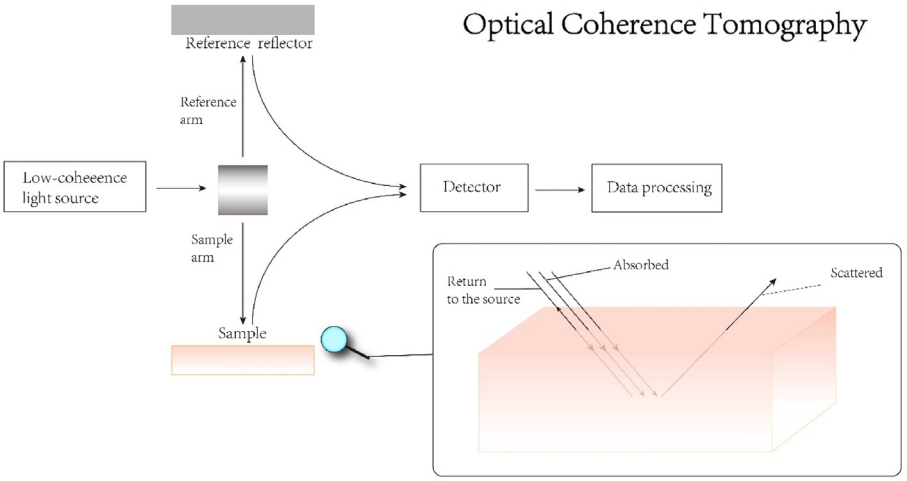

Scheme 2. The light from the source is divided into two paths, namely the two arms of the interferometer (the reference arm and the sample arm). In the reference arm, the mirror reflects light. In the sample arm, light has three paths, scattering, absorbing and returning to the source (backscattering). By comparing and analyzing the backscattered light signal of the sample arm and the reference arm, the image is finally obtained.

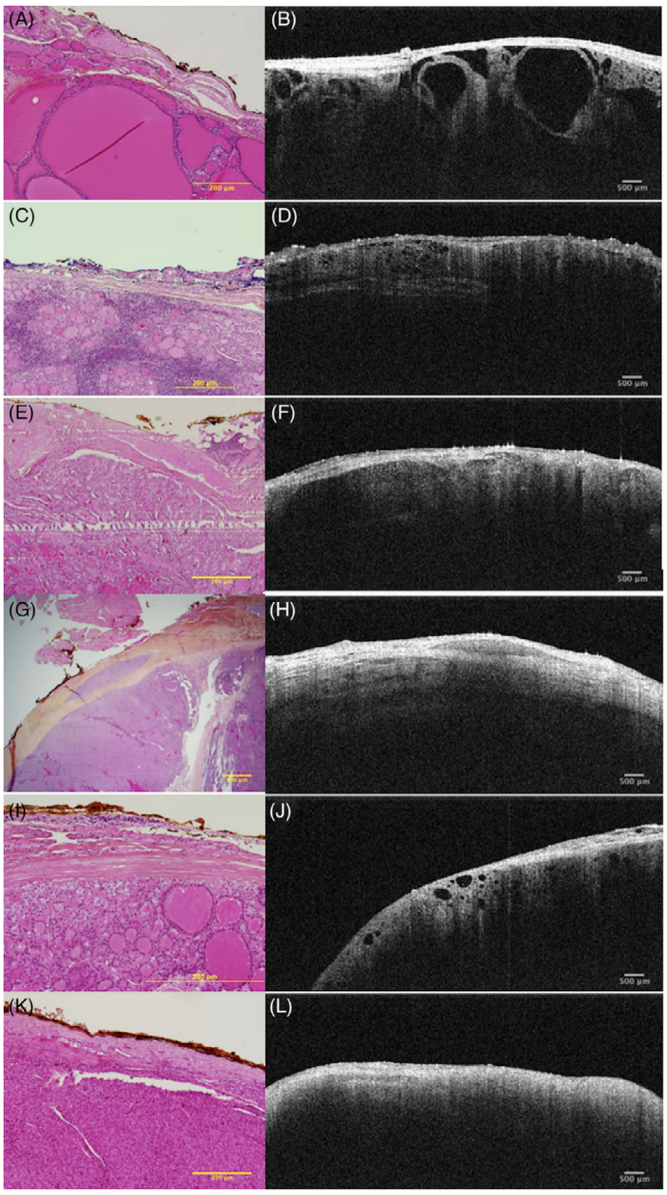

Fig. 1. Hyperplastic nodules (A & B); lymphocytic thyroiditis (C & D); classic variation of PTC (E & F); solid variant of PTC (G & H); follicular variant of PTC (I & J); and thyroid adenoma (K & L) histological and OCT appearances [37] (Reproduced from Ref. [37] with permission. Copyright 2019 Wiley Periodicals, Inc.).

indirect diagnosis of thyroid disease. The strong correlation is well documented between aberrant Selenocysteine (SEC) levels and a number of disorders, including thyroid, cardiovascular, diabetic, and neurodegenerative diseases [29–31]. In thyroid diseases, SEC and H_2O_2 levels are negatively correlated. A potential chemical diagnostic for the detection of TC, the radiometric NIR fluorescence probe (Mito-Cy-SEC) was devised and synthesized in research [32]. It allows for the observation and analysis of SEC alterations in thyroid disease-related cell lines and mouse models. A few advanced but inexpensive fluorescent probes can detect tumor-associated markers in vivo with high sensitivity and high infectivity [33,34], which may open a new era of TC diagnosis.

2.2. Optical Coherence Tomography (OCT)

By combining high longitudinal resolution with a high lateral resolution, OCT, a non-contact, non-invasive, and non-damaging imaging

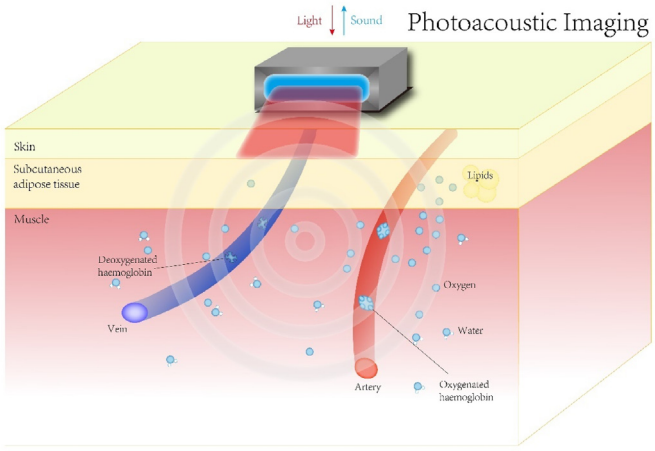

Scheme 3. Using different wavelengths of near-infrared light to illuminate the tissue, the ultrasound signal is generated after different light pulses. Photoacoustic images are generated by the reconstruction of photoacoustic signals.

technology, may provide data that is comparable to that of tissue pathology (Scheme 2). OCT uses a low-energy NIR light source as the detection light and combines a microscope head, a handheld probe, or an endoscope for routine detection in a non-invasive manner without causing damage to biological tissues. Recent research suggests that the OCT technology may evaluate follicle shape and demonstrate thyroid tissue growth patterns [35,36] (as shown in Fig. 1 [37]), which may also lessen the frequency of fine needle aspirations (FNAs) carried out in benign nodules in multinodular colloid goiter. OCT has since become a helpful supplementary tool in the identification of malignant and benign thyroid nodules and may be able to decrease the need for FNAs by eliminating nodules with clear signs of benignity. The potential rate of false positive diagnoses will be reduced, and the number of nodules requiring further testing for evaluation will be decreased, which will aid in lowering the costs of unnecessary testing for thyroid nodules that were unintentionally discovered. OCT is simple to operate, with short imaging time and high resolution. However, the limited imaging depth of OCT, generally limited to 2 mm, is the biggest obstacle that hinders its translation into clinical diagnostic applications.

2.3. Photoacoustic imaging (PAI)

In contrast to previous optical imaging modalities, photoacoustic imaging (PAI) is a hybrid imaging modality that has emerged in recent years that combines laser and ultrasound detection, taking advantage of the optical properties of sensitive tissues [25] through high ultrasound resolution and strong optical contrast. Photoacoustic imaging uses instantaneous light to irradiate the tissue. Molecules in the tissue produce different degrees of rapid expansion under excitation light of different wavelengths, so as to generate ultrasonic waves that are detected by the ultrasonic detector. The depth is determined by different ultrasonic signal time. The image is reconstructed through data processing to form an image (Scheme 3). The depth of imaging and resolution of PAI is inversely proportional to the frequency of the ultrasound detector used (e.g., a center frequency of 4–6 MHz and a bandwidth of 0.1–10 MHz for an imaging depth of 2–4 cm) [38]. PAI is one of the hot spots of novel diagnostic modalities being explored for various systemic diseases, such as the quantitative functional evaluation of liver fibrosis in mice by photoacoustic imaging explored by Jing Lv et al. [39]. Based on the light absorption properties of certain substances in the body (e.g., hemoglobin and lipids, etc.), PAI displays key functional data, such as oxygen saturation, and detect small vessels that are not detected by color Doppler ultrasound [38,40]. PAI demonstrating the presence of hypoxia and reduced lipid content in malignant thyroid nodules compared to benign

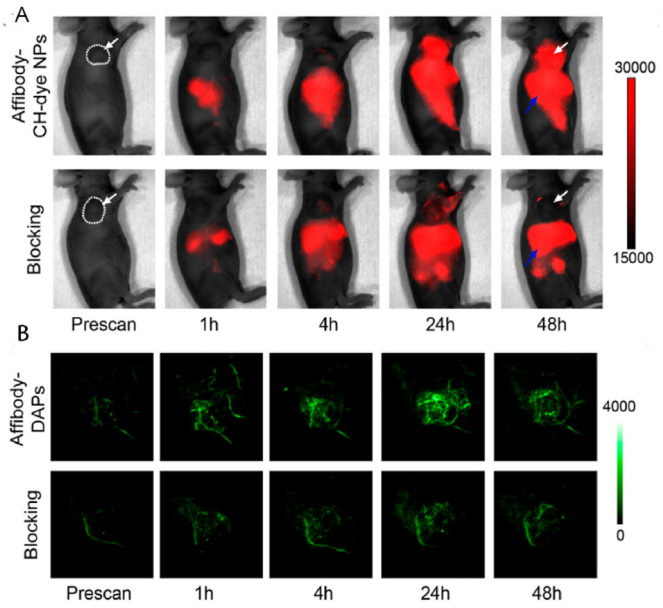

Fig. 2. Dual-mode imaging (PAI combined with FI). The NIR-II fluorescence images (A) of epidermal growth factor receptor (EGFR)-positive FTC-133 tumor-bearing mice were captured before injection and 1, 4, 24, and 48 h after tail vein injection of Affibody-DAPs, respectively. The blocking group was co-injected with Affibody ZEGFR:1904 and Affibody-DAPs. (Images of both groups using the same acquisition parameters.) Coronal views of the 3D volume rendering of the PAI (B) of the FTC-133 tumors were obtained at the predefined time intervals right after FI. White dashed lines and white arrows indicate tumors [25] (Reproduced from Ref. [25] with permission. Copyright 2017 American Chemical Society).

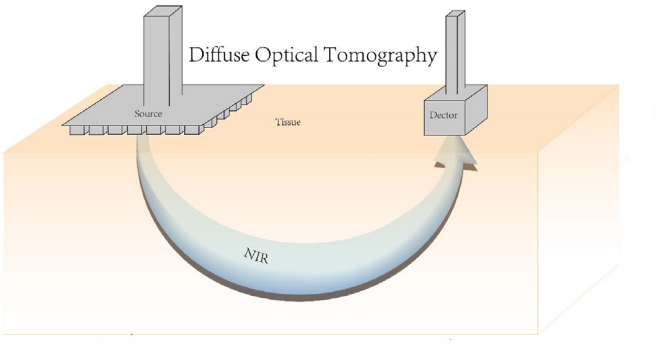

Scheme 4. Schematic diagram of diffuse optical tomography.

thyroid nodules can aid in the diagnosis of TC, which has unique advantages over traditional screening diagnostic modalities for thyroid disease. In addition to providing structural support and giving functional information, PAI can potentially distinguish benign and cancerous thyroid nodules from healthy thyroid tissue using multispectral PAI. Eighty-eight thyroid sections from 50 patients yielded great results. Sensitivity, specificity, positive predictive value and negative predictive value of PAI in differentiating malignant and benign thyroid lesions were 69.2%, 96.9%, 81.8% and 93.9%, respectively [41]. More importantly, PAI possess the advantage of having no binding barriers and can be integrated with other imaging modalities to create a multimodal imaging platform, such as with ultrasound imaging or NIR-II fluorescence imaging (Fig. 2) [42–44], all of which have shown excellent capabilities in the diagnosis of TC. Overall PAI can provide images of thyroid structures and functional information such as vascularity, oxygenation and inflammation without ionizing radiation or injection of exogenous contrast agents, and with a short examination duration (~5 min), it has great potential for clinical translation.

2.4. Diffuse optical tomography (DOT)

DOT is a thick tissue imaging technique that typically collects light scattering information in the near-infrared spectral range and then analyzes it through statistical models in order to obtain three-dimensional images with an imaging depth of roughly 1–1.5 cm [45,46], promising a non-invasive diagnosis of TC. Traditional DOT requires a high-density array of probes to capture a large amount of biological information in order to reveal biological 3D information, which is very time-consuming (Scheme 4). Some researchers have proposed a novel DOT system that uses a multi-directional emitting light source and a photodetector to replace the traditional high-density probe array, ultimately achieving an imaging depth of 1.5 cm [46]. Whether a high-density probe array combined with multi-directional measurements can obtain satisfactory DOT images while reducing imaging time is to be further explored by researchers. A study claims that DOT can assist in the diagnosis of FTC by detecting the degree of tumor hypoxia [47]. However, the nature of light scattering, refraction and absorption during propagation, and the structure of the thyroid gland adjacent to the trachea and large blood vessels make it more difficult to obtain high-quality images like CT. Some studies have attempted to establish DOT imaging models to reduce the above-mentioned interference [47,48], but there is still a long way to go for thyroid DOT 3D image establishment. Research on the effectiveness of DOT for TC diagnosis and treatment is still in its early stages.

3. Phototherapy in TC

3.1. Photothermal therapy (PTT)

The highly aggressive and treatment-resistant nature of undifferentiated TC [49,50] makes its prognosis extremely poor. Traditional surgery and radiotherapy have little effect on undifferentiated TC and are often associated with numerous complications. The advent of NIR imaging combined with phototheranostics has brought hope to both patients and physicians, as it not only provides a clear diagnosis but also allows targeted localized killing of tumor cells with minimal or no damage to surrounding organ cells.

With benefits of being manageable, non-invasive, and having minimal side effects, PTT is a therapy approach that employs photothermal reagents (PTA) to transform light energy into heat energy for tumor cell ablation under proper external light irradiation [51]. Some of the nanoprobes applied in NIR imaging tend to have good photothermal conductivity, allowing some of them to be used as PTAs in PTT. Meanwhile, by purposefully processing and modifying PTA, they can specifically target certain tumor cells. The following probes can all greatly improve the thermal efficacy (Fig. 3) on thyroid tumor cells, achieving precise local thermal ablation of tumors with no significant cytotoxicity observed in animal experiments: Polymeric NPs with bevacizumab and IR825 conjugated on the surface (IR825@B-PPNs) [52], ^{131}I-radio-labeled cerebroid polydopamine nano-particles (CPDA-^{131}I NPs) [53], ^{131}I-labeled BSA-modified CuS nanoparticles (^{131}I-BSA@CuS) [54], meso-methoxy-substituted DSPE-PEG-2000-coated boron dipyrromethene (B–OMe-NPs) [55], polypyrrole (Ppy)−poly-(ethylene imine)−siILK nanocomplex (PPR_{ILK}) [56], functionalized (epidermal growth factor (EGF), holo-transferrin, or lapatinib) HAOA-coated AuNPs [57], and photo-triggered Gold nanodots capped mesoporous silica nanoparticles (Au@MSNs) [58] (Table 2).

The two energy dissipation modalities of PTT and FI are in conflict with one another since energy is conserved. Therefore, the goal of NIR-guided PTT is to develop a method to balance photothermal effects (non-radiative decay) with fluorescence (radiative decay) [59]. Additionally, hyperthermia-induced inflammation might raise the danger of cancer recurrence. PTT in combination with anti-inflammatory medication would thus be more sensible and efficient. According to reports,

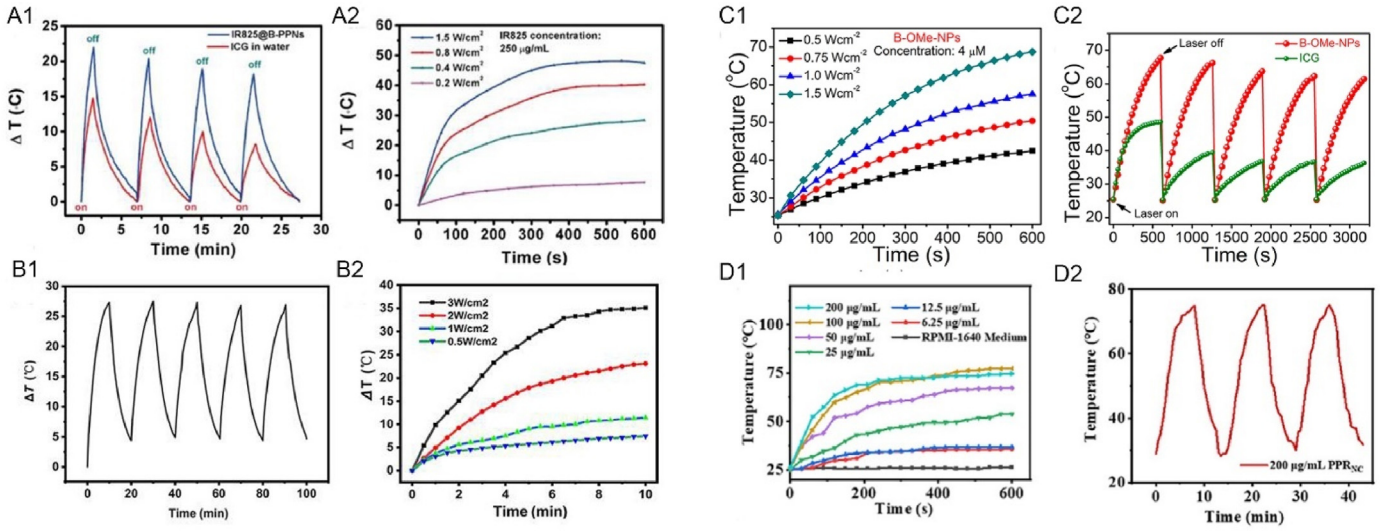

Fig. 3. Thermal efficacy of IR825@B-PPNs (A), CPDA-^{131}I NPs (B), ^{131}I-BSA@CuS (C), B–OMe-NPs (D), PPR_{ILK} (E) [52–56]. The temperature fluctuation curves of the indocyanine green (ICG) solution and IR825@B-PPNs after four photothermal heating cycles (A1). The different power-density irradiation (A2) (Reproduced from Ref. [52] with permission. Copyright 2019 Acta Materialia Inc. Published by Elsevier Ltd). The five photothermal cycles of BSA@CuS's temperature fluctuations (B1). The images of the photothermal heating curve at various light intensities (B2) (Reproduced from Ref. [54] with permission. Copyright 2022 International Union of Biochemistry and Molecular Biology). Time-dependent temperature variation of B–OMe-NPs at different laser powers (C1). Photothermal cycle of BOMe-NPs and ICG solutions during laser irradiation (C2) (Reproduced from Ref. [55] with permission. Copyright 2022, American Chemical Society). Heating curves of PPRNC in gradient concentrations during 10 min of laser irradiation (D1). Temperature changes in PPRNC during three laser irradiating and natural cooling-down cycles (D2) (Reproduced from Ref. [56] with permission. Copyright 2022, American Chemical Society). (For interpretation of the references to colour in this figure legend, the reader is referred to the Web version of this article.)

hydrogen has a significant advantage in minimizing tissue inflammation brought on by high temperatures. Therefore, the NIR-controlled hydrogen nanoplatform combined with PTT would be a feasible solution. The reported PdH0.2 nanocrystals [60] and the hydrogenated Pd-MOF (porphyrin–palladium metal–organic framework) [61] exhibited good controlled hydrogen release properties and photothermal effects, which have been confirmed.

3.2. Photodynamic therapy (PDT)

PDT activates photosensitizers by laser light at specific wavelengths, which in turn releases a highly reactive free radical oxygen molecule that causes necrosis of cancer cells, especially the blood vessels that nourish cancer cells [51,62]. PDT's three basic components are photosensitizer, light source, and oxygen [63]. PDT is an excellent non-invasive tumor treatment with the advantages of fewer side effects, a strong ability to kill tumor cells, and not interfering with the application of other treatments [62]. However, the tumor's microenvironmental hypoxia and lack of targeting limits its further clinical application. There are two main approaches to solving the former problem: (1) delivering oxygen directly to the tumor region through a carrier [64,65]; (2) generating oxygen through biochemical reactions at the tumor site [66,67]. In addition, the problem of weak targeting can be solved by chemical modification of photosensitizers or the construction of nanosystems containing targeting ligands.

An excellent nanosystem, consisting of a combination of tumor-recognizing specific molecules, photosensitizers, and NIR fluorescent probes, can achieve precise imaging diagnosis and local killing of tumor cells when activated by NIR light and has great potential to be applied to the treatment of TC. It has been demonstrated that the application of porphyrin-HDL nanoparticle (PLP)-mediated PDT in preclinical models of TC can achieve specific ablation of thyroid tumors, preserving normal thyroid tissue without tracheal or nerve damage [68] (Table 3). In addition, chemotherapy combined with PDT can obtain better inhibition of thyroid tumor growth and induction of tumor cell apoptosis [69,70]. The reason may be that PDT contributes to the internalization of chemotherapeutic drugs [70]. Photosensitizers that are currently being investigated are those such as Hypericin [71] (Table 3), a natural photosensitizer, which when combined with PDT can achieve excellent destruction of thyroid tumor cells by inducing intracellular reactive oxygen species (ROS) production and mitochondrial damage. The most interesting aspect that has attracted the attention of researchers is the multimodal imaging of PDT. For example, Xuejian Xing et al. developed a nano-therapeutic platform integrating NIR-FI, PAI, PTT and PDT, which has the potential to realize the application of NIR-FI and PAI for co-guided PDT and PTT treatment.

In practical clinical applications, it is difficult to obtain satisfactory efficacy with PTT or PDT alone because of the heat shock effect in PTT and the hindrance of the hypoxic tumor microenvironment in PDT [72,73]. Thus, combining two treatments may be a promising solution. PTT enhances the effect of PDT by increasing the blood flow rate to increase the oxygen concentration in the tumor microenvironment, and this effect in turn promotes the elimination of heat-resistant tumors in PDT [59]. In addition to PTT, other treatment modalities can also be integrated into the nanotherapy platform according to the patient's specific conditions. As illustrated in Fig. 4 [74], the four treatment modes, including H_2, PDT, PTT, and enhanced chemodynamical therapy (ECDT), can be combined on a single nanoplatform to constitute an H_2-mediated cascade of amplified synergistic therapies. Multimodal treatment nanoplatforms are very promising in the treatment of cancer.

In conclusion, PDT and PTT have their unique advantages over traditional tumor treatment modalities (e.g., surgery, radiofrequency ablation, radiation therapy, chemotherapy, etc.). The design of targeted optical probes and the control of laser irradiation together ensure the precision of phototherapy and minimize the toxic effects that deviate from the target tumor to the surrounding tissues. Non-invasiveness is also one of the great advantages of phototherapy, as surface organs can be treated with non-invasive laser irradiation to stimulate PTT or PDT, while deep organs can be treated with intervention techniques like fiber optic and endoscopic to allow avoidance of dissection and chest opening. Phototherapy is extremely biocompatible and can be safely used multiple times intra-human. Meanwhile, phototherapy has considerable potential

Table 2
PTT performance of various NIR probes supported by existing literature [52–54, 57,58].

PTA	Performance	Application	Indication
Bevacizumab (antibody) and IR825 [52]	The treatment efficiency of tumor eradication by near infrared (NIR) laser irradiation was significantly improved.	Build a sequentially targeted nanoplatform (IR825@Bev-PLGA-PFPNPs) for PTT.	ATC
mesoporous polydopamine nanoparticles (MPDA) [53]	Porous nanoparticles show huge advantages in the field of drug delivery, which can effectively improve the loadings of chemotherapeutic drugs or other substances.	MPSNs were used as nanocarriers for loading various drug molecules by virtue of their open pore structure and adjustable pore channels to treat cancer.	ATC
the ^{131}I-labeled BSA-modified CuS nanoparticles (^{131}I-BSA@CuS) [54]	The synthesized nanomaterial showed uniform dispersion, good stability and aqueous solubility, excellent photothermal properties, and long-term retention in ATC.	As a therapeutic agent, it has shown remarkable efficacy in both ACT radiotherapy and PTT.	ATC
B–OMe-NPs [55]	B–OMe-NPs and laser irradiation mediated therapy and cell proliferation inhibition lead to tumor tissue damage	It has good photostability and effective photoacoustic imaging and fluorescence imaging ability, and combines PTT and PDT treatment modes	Cancer
Based on a polypyrrole (Ppy)-poly-(Ethylene imine)-siILK nanocomplex (PPR_{ILK}) [56]	Tumors were completely eradicated by photothermal therapy, and the recurrences and metastases were obviously restrained by siILK	It has excellent biocompatibility and stability, and can be modified by surface to achieve charge reversal to load and release siILK under appropriate conditions.	PTC
holo-TRANSFERRIN, (EGF and lapatinib-functionalized AuNPs (gold nanoparticles) [57]	AuNPs have many advantages, including efficient light-heat conversion and tunable optical properties that can be manipulated by varying the AuNPs's physical characteristics such as size and shape.	For PTT, nanotechnology can change the photothermal properties of the medium and enhance tumor hyperthermia.	ATC
Photo-triggered Gold nanodots capped mesoporous silica nanoparticles Au@MSNs [58]	The capsaicin and Cap-AuMSNs were able to inhibit the migration and invasion of cancer cells.	For PTT, Cap-AuMSNs are in the nano regime and highly stable.	TC

to be used in combination with other therapies, such as chemotherapy and immunotherapy. With the advanced research on phototherapy, an increasing number of multifunctional probes are demonstrating superior optical properties. However, multifunctional advanced targeting probes may lead to difficulties in chemical preparation and quality control, limiting their translation to the clinic. The clinical application of a technology requires not only the assurance of its therapeutic efficiency, but also the consideration of its preparation, preservation and transportation costs, along with the practicality of the control system and the selection of the target tumor. Thus, phototherapy is a very promising but complex subject that has the potential to move forward as a next-generation of oncology treatment technology.

Table 3
PDT performance of various NIR probes supported by existing literature [68,71].

Photosensitizer	Performance	Application	Indication
The porphyrin-HDL nanoparticle (PLP) [68]	Providing a safe, minimally invasive, and effective alternative to thyroidectomy for TC therapies	PLP-PDT enabled complete ablation of tumor tissue while sparing both the normal thyroid tissue and RLN from damage.	DTC
Hypericin (HYP) [71]	HYP, isolated from St. John's wort (*Hypericum perforatum* L), is regarded as a powerful photosensitizer, which is studied for its photodynamic effects.	HYP-assisted PDT can promote mitochondrial damage and cell apoptosis in adenocarcinoma, liver cancer, and vascular malformation cells.	ATC
B–OMe-NPs [55]	B–OMe-NPs and laser irradiation mediated therapy and cell proliferation inhibition lead to tumor tissue damage	It has good photostability and effective photoacoustic imaging and fluorescence imaging ability, and combines PTT and PDT treatment modes	Cancer

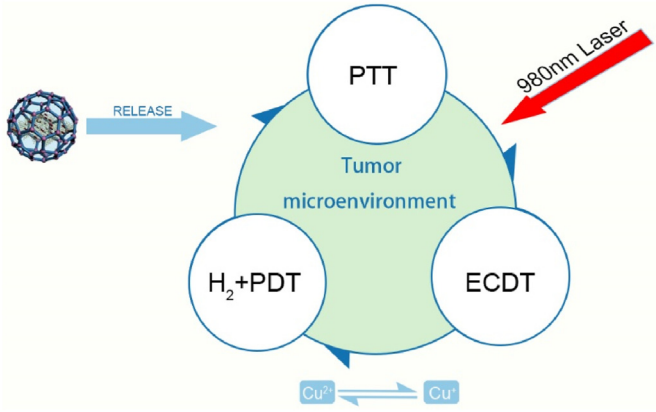

Fig. 4. The schematic representation of the multimodal nano-platform: H_2 mediated cascade enhancing synergetic treatment [74].

4. Combined treatment for TC

4.1. *Radiotherapy & chemotherapy*

RIT has been available throughout the past sixty years and usually exists as a complementary treatment to surgical treatment. DTC Patients with a high risk of recurrence have benefited from utilizing RIT, whereas DTC patients with low risk have not benefited from its effects on tumor-free and final survival [75]. Even while RIT is often well tolerated, it may have a number of short- and long-term harmful adverse effects [76]. Some studies have attempted to combine ^{131}I radiation therapy with PTT in TC [54,77]. RIT is now being widely employed in the treatment of TC. Compared with single treatment, the combination of radiation therapy and PTT has stronger anti-tumor activity, and no significant toxic side effects were observed in animal experiments, so the clinical application is promising.

Since chemotherapeutic drugs have a propensity to destroy both tumor cells and healthy cells without discrimination, chemotherapy is not frequently employed in DTC. In contrast, for undifferentiated TC,

radiation therapy and chemotherapy are often combined with surgery. The American Thyroid Association guidelines recommend docetaxel/paclitaxel and platinum in ATC, despite yielding no benefit to survival in advanced ATC [78]. One of the key problems preventing the successful treatment of malignant tumors is multidrug resistance (MDR) [79]. The construction of nanoparticles for precise targeted delivery of chemotherapeutic drugs is expected to solve this problem, and the construction of optical diagnostic imaging, phototherapy, and chemotherapeutic drug delivery in a multimodal nanoplatform has become a popular topic for research. According to one study, carboplatin (CBDCA) and PDT together may more effectively inhibit tumor development and trigger apoptosis in anaplastic TC via modulating EGFR and PI3K as well as activating PTEN [70]. PLGA-Au-TiO2@CPT-11 and PLGA-Au-TiO2@CPT-11 + NIR nanoparticles have shown excellent antimetastatic characteristics and decreased cell invasion activity in B-CPAP and FTC-133 TC cell lines [79]. We believe that targeted photoexcitation to control the precise release of chemotherapeutic agents, complemented by phototherapy and real-time imaging of tumors can together propel chemotherapy into a new phase.

4.2. RNA therapy

RNA therapy has been extensively researched and developed as a novel diagnostic and therapeutic tool for cancers. The thermodynamic stability and specific targeting of RNA offer the possibility of RNA therapy, which reduces the oncogenic properties of cancer cells by overexpressing cancer-specific genes through small interfering RNA (SiRNA), resulting in apoptosis of cancer cells [80]. The prognosis for ATC, a thyroid subtype, is quite poor, and standard therapies, including surgery, radiation, and chemotherapy, have not been very effective. V-Raf murine sarcoma viral oncogene homolog B (BRAF) mutations are present in 40% of ATC patients, while additional MAPK pathway mutations (downstream of BRAF) are present in 20%–40% of ATC cases. Yanlan Liu et al. designed a NIRF nanoplatform for imaging metastatic ATC combined with RNA therapy [81]. It has been demonstrated that the group's newly created NIR nanoplatform can make it easier to introduce siBRAF into ATC transplant tumors in vivo. This will cause strong BRAF silencing in the tumor tissues and will effectively stop the growth of the tumor without causing any discernible side effects. Experimental investigations showed the capacity to cause lengthy circulation and substantial tumor accumulation in both xenograft and in situ ATC models (Fig. 5). More remarkably, the systemic administration of siBRAF-carrying NIR nanoparticles dramatically decreased the incidence of intrapulmonary micro-metastases. We believe that excitation by optical localization can achieve aggregated release of siRNA, and may increase the targeting and promotion of cancer cells into programmed death, making it a very promising diagnostic and therapeutic option for malignant tumors. However, its clinical translation needs to overcome the shortcomings of RNA biological instability and short circulating half-life [82]. Experimental data related to RNA therapy combined with optical imaging/therapy for TC are still lacking, and only a few RNA-based nanoparticles of other systems have entered clinical trials. Thus, we expect more research results to emerge.

4.3. Optical imaging-guided surgery

Real-time feedback and the availability of reasonably priced video systems that provide a broad view of the surgical field are two potential benefits of OI [83]. Therefore, the application of OI technology to surgery will enhance the surgeon's preoperative and intraoperative visualization and improves the accuracy of postoperative assessments, facilitating integration into the daily clinical surgical operation process.

4.3.1. Lumpectomy guidance

Surgery is one of the treatments of choice for the vast majority of solid tumors. Traditional imaging techniques are difficult to apply in the operating room due to low temporal or spatial resolution, cumbersome and large imaging instruments, and poor timeliness [22]. NIR imaging, characterized by high temporal and spatial resolution molecular imaging, has received tremendous focus from researchers. In the last decade, NIR-II imaging with less light scattering, deeper penetration depth, and higher signal-to-noise ratio of imaging [84,85] compared to NIR-I imaging, has shown great potential for clinical applications. The U.S. Food and Drug Administration (FDA) has approved a number of NIR fluorescent dyes (indocyanine green (ICG), 5-aminolevulinic acid (5-ALA), and methylene blue) and imaging systems for diagnostic and therapeutic applications [86–88]. Among them, ICG has been extensively utilized in clinical applications, including tumor imaging, lymph node imaging, angiography, and tissue perfusion, by virtue of its good biosafety and superior optical properties. ICG, as a NIR-II imaging dye, has been widely applied in tumor resection evaluation. ICG-based tracers can be localized in real-time, effectively and precisely, reducing the chances of missing or mistakenly injuring normal thyroid tissue or important anatomical structures around the thyroid, and maximizing patient prognosis based on complete resection of tumor tissue. It has a high application value in the surgical resection of primary and recurrent tumors in the head and neck [89–91]. Tissue factor (TF) is a prospective diagnostic marker for a number of malignancies, including breast, pancreatic, and TC, among others, according to recent research. A study [92] developed IRDye 800CW-ALT-836 (Fig. 6) based on TF-specific monoclonal antibodies, is a fluorescent dye with superior targeting ability, which showed preliminary effectiveness in preclinical mouse models for the diagnosis and treatment of ATC, facilitating complete in situ resection of ATC tumors. NIR-FI is the most clinically promising OI modality for real-time surgical navigation, assisting surgeons in the complete removal of tumors while minimizing surgical complications.

A study concluded that oct can differentiate between benign, malignant, and normal thyroid tissue in ex vivo specimens [35]. It has also been shown to be able to distinguish the thyroid and parathyroid glands [37]. The capacity of OCT to conduct real-time surgical navigation during an operation has also been demonstrated [93,94]. According to research [36], in ex vivo thyroidectomy specimens of patients who had undergone surgical excision for the therapy of PTC, optical biopsy employing OCT is a viable alternative to frozen sections for the diagnosis of microscopic extrathyroidal extension (mETE). Using a changing axis of laser scanning, OCT can show high-resolution real-time pictures of the tumor and surrounding envelope in this preliminary study [36]. OCT is simple to use

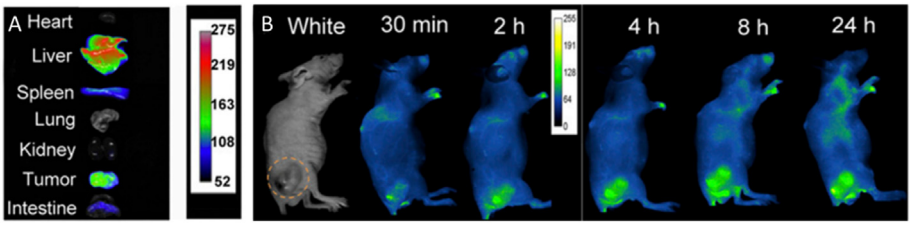

Fig. 5. In vivo NIR imaging of organs from B (A). After receiving a single dosage of NIR NPs, a BRAFV600E-mutated 8505C tumor-bearing animal showed time-dependent FI (B) [81] (Reproduced from Ref. [81] with permission. Copyright 2022 National Academy of Science).

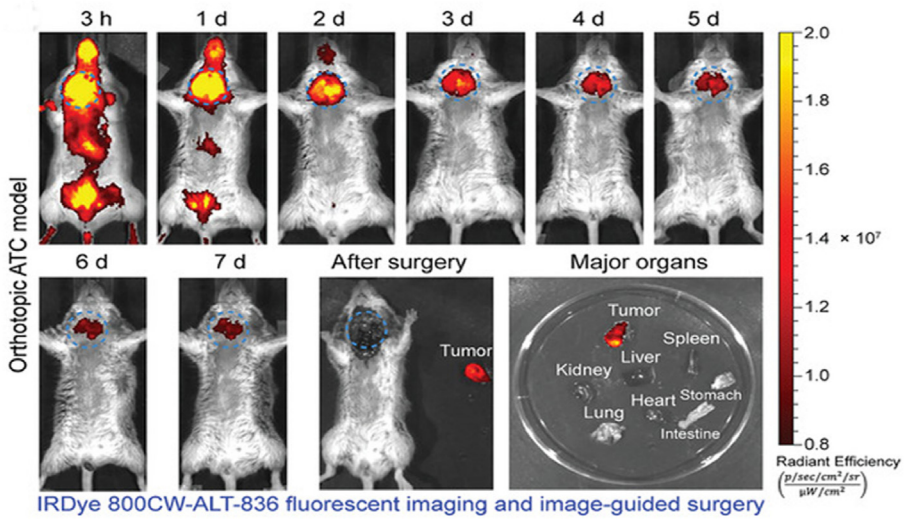

Fig. 6. Serial FI following injection of IRDye 800CW-ALT-836 and image-guided tumor removal seven days later. In vitro fluorescent imaging, strong fluorescent signals were seen in the tumor, but not in the other organs. Blue dashed circles indicated the tumor [92] (Reproduced from Ref. [92] with permission. Copyright 2020 The Authors. Published by WILEY-VCH Verlag GmbH & Co. KGaA, Weinheim). (For interpretation of the references to colour in this figure legend, the reader is referred to the Web version of this article.)

and may be completed in 3 min or less on average. OCT may eventually be able to do intraoperative "optical biopsies" without the need for fixation, staining, or tissue removal with further advancements in OCT miniaturization and intraoperative sterile probe formats. However, OCT imaging can only penetrate as deep as 1–2 mm, hence intraoperative thyroid imaging is only possible on the exposed surface and superficial tissue.

4.3.2. Mapping metastatic lymph nodes

Lymph node dissection is a critical component of radical TC surgery. The extent of lymph node dissection is still in disagreement, but there is a general consensus that dissection at minimum should cover the central zone (zone VI), since it is often the first station of TC lymph node metastasis. A series of problems, including laryngeal return nerve damage and hypoparathyroidism, can result from over-treating prophylactic lymph node dissection [95]. NIR fluorescence-guided lymph node dissection can reduce these problems to a large extent.

A clinical study [96] found that PTC nodal metastases had a stronger fluorescence intensity than healthy lymph nodes ($p < 0.0001$) and fat/-connective tissue ($p < 0.0001$) (Fig. 7), confirming that EMI-137 was primarily aggregated in the cytoplasm of TPC1 cell lines and PTC nodal metastases and that the near-infrared fluorescence (NIRF) tracer was internalized in MET-positive cells. The use of NIRF tracer (EMI-137) in the perioperative period to detect PTC lymph node metastases is safe and feasible and may reduce the negativity of prophylactic central compartmentalized node dissection (CLND), ultimately minimizing the incidence of overtreatment and complications during PTC lymph node dissection. NIR imaging to identify metastatic lymph nodes of TC using fluorescent probes formed by ICG as the basic backbone with targeted functionalization modification is one of the very promising methods that can be applied to surgical navigation to reduce excessive lymph node dissection. For example, the ICG-99mTc-nanocolloid combination designed by Nilda Sütay Süslü et al. [90] and a combination of ICG and carbon nanoparticles (CNs) designed by Xing Zhang et al. [97] have been shown in clinical studies to more accurately identify metastatic lymph nodes. This can provide precise clinical staging and lymph node dissection to improve the prognostic survival quality of patients.

Real-time intraoperative lymph node imaging screening is limited by the 1–2 mm imaging depth of OCT. However, Erickson-Bhatt, Sarah J et al. [93] suggested that in the future, portable intraoperative systems with OCT needle probes could allow in vivo imaging of the surgical cavity and exposed local area lymph nodes after the removal of the tumor. The ability to differentiate between metastatic lymph nodes and healthy lymph nodes has been shown to depend on the nuclear characteristics of papillary TC cell inclusion bodies seen inside the lymph node parenchyma (Fig. 8) [37], which manifests as the lack of homogenous parenchyma on OCT. The primary characteristic that distinguishes metastatic lymph nodes from normal lymph nodes on OCT is the lack of homogenous parenchyma. It was observed in 78% (14/18) of metastatic lymph

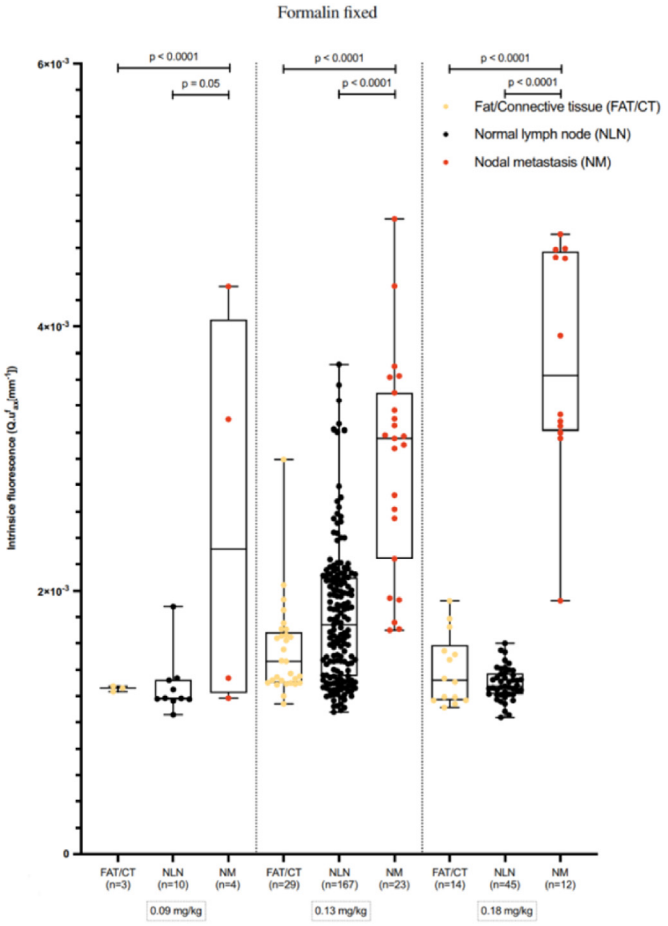

Fig. 7. A description of the intrinsic fluorescence observed in both normal lymph nodes and formalin-fixed PTC nodal metastases under quantitative spectroscopy conditions [96]. (Reproduced from Ref. [96] with permission. Copyright 2022 The Author(s). Published by Springer Nature).

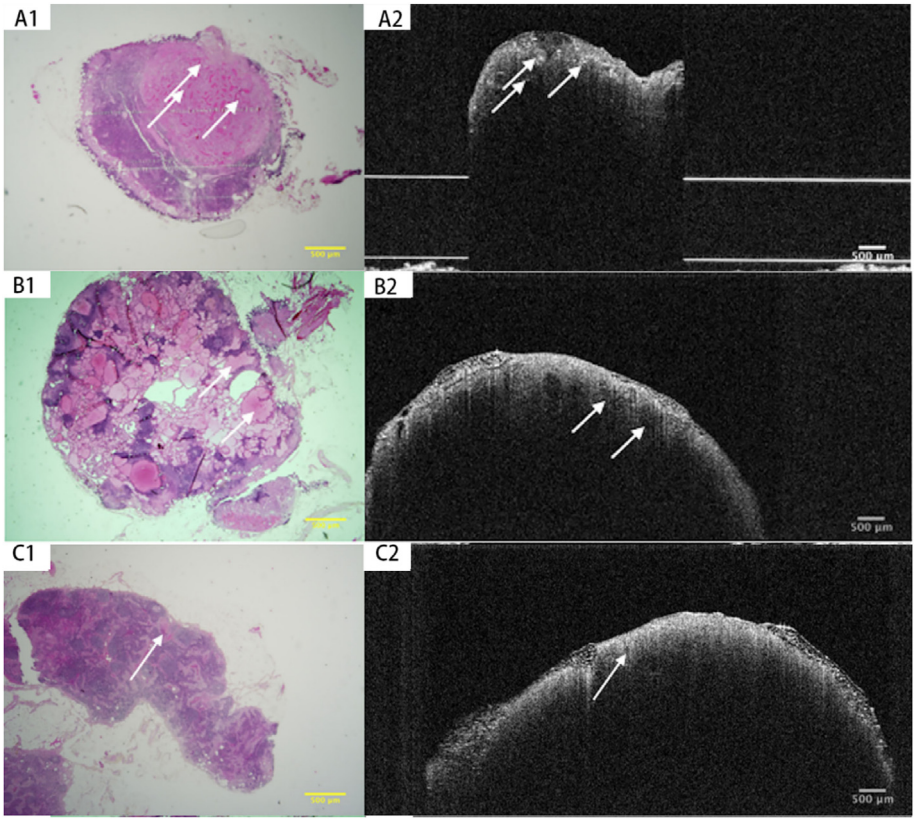

Fig. 8. Papillary architecture (A1 & A2) (arrows) and follicular architecture (B1 & B2) (arrows) are observed in histological and OCT appearances of metastatic PTC to lymph nodes. Homogeneous parenchyma and vessels (C1 & C2) (arrow) are observed in histopathological and OCT of the benign lymph node [37] (Reproduced from Ref. [37] with permission. Copyright © 2019 Wiley Periodicals, Inc).

nodes [37]. Images of lymph nodes and parathyroid adenomas could be misinterpreted for one another, failing to discriminate between benign and malignant thyroid nodes.

PAI has not been explored for the early diagnosis and treatment of TC micrometastases. However, its significance has been reported in other diseases, such as in the work of Qian Yu et al. where PAI was concluded to be able to detect in vivo melanoma liver micrometastases up to 7 mm deep with a size of approximately 400 μm. This is more sensitive than the capabilities of that of ultrasound and MRI [14]. Due to its excellent penetration depth and sensitivity for metastasis identification, we can foresee that PAI will have the potential to be an excellent media for surgical navigation.

4.3.3. *Identifying parathyroid gland*

TC surgery can often be accompanied by numerous complications. Due to accidental excision of the gland or damage to the blood vessels supplying the parathyroid glands, hypoparathyroidism is the most prevalent complication following total or almost total thyroidectomy. According to reports, the percentage of lifelong hypoparathyroidism ranges from 0.4 to 13.8% [11] and may reach 37% in cases of bilateral neck dissection for thyroid malignancy [98].

NIR imaging is very effective in preventing hypoparathyroidism to be believed by most surgeons, because it can be applied to examine the parathyroid glands (PGs) during TC surgery and determine if the blood supply to the glands is compromised [99]. The application of NIR imaging techniques in the prevention of parathyroid injury is divided into two main categories: (1) Imaging of parathyroid autofluorescence; (2) FI with exogenous tracers (e.g., ICG).

By visualizing the parathyroid glands (Fig. 9 shows the green ICGA fluorescence of the residual parathyroid glands [100]), NIR fluorescence-guided surgery is an effective, feasible, and safe method to reduce the incidence of post-thyroidectomy hypoparathyroidism. It reduces the risk of postoperative hypoparathyroidism and hypocalcemia as a result of fluorescence-guided surgical research to be able to improve the early detection, visibility, and preservation of PGs in addition. This imaging method also aids in locating unintentionally removed glands on samples for later autologous transplantation [99]. During thyroid surgery, OCT can be used as a device to assist identifies parathyroid glands. According to studies [37,99,101–103], OCT imaging's qualitative criteria may be utilized to identify and preserve parathyroid glands during thyroidectomy, and the procedure has no side effects or radiation emissions. However, a study [104] observed a marginally better vision of the gland in white light, presumably because the strong background signal of the hypervascularized tumor tissue interfered with the imaging of FI. Research including 542 patients show no discernible difference in the number of visualized PGs between the NIR autofluorescence and conventional groups [105], because of the surgeon's extensive experience.

4.3.4. *Identification of the thoracic duct*

When performing lymph node dissection in zone IV, the thoracic duct is not readily identifiable and is very vulnerable to injury, leading to celiac leakage. So far, there has been no conventional technique for the identification of intraoperative auxiliary thoracic duct (TD). Previous cases have reported the use of ICG for TD identification in the thorax and abdomen in humans [106–108]. One study [109] performed ICG NIR imaging intraoperatively and postoperatively in six patients who underwent left cervical lymphatic dissection (grade II-IV) for TC or melanoma (typical FI is shown in Fig. 10), demonstrating that ICG identification of TD is technically feasible and has the potential to be an important adjunct for surgeons. It will also help to identify the location of the injury and confirm the completion of the repair when intraoperative celiac fluid leakage is observed. Nevertheless, limited by the depth of

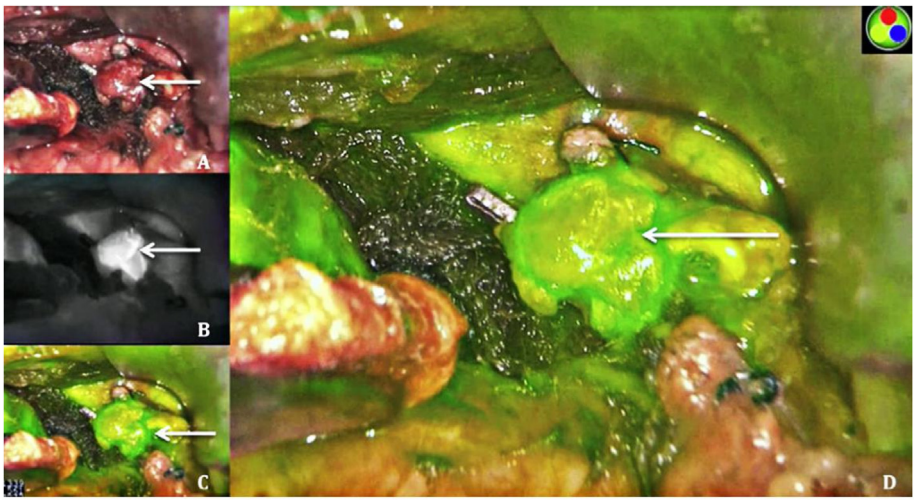

Fig. 9. Patient undergoing subtotal parathyroidectomy. Residual parathyroid gland (arrow) (A). Greyscale ICGA demonstrating excellent residual perfusion (B). Green ICGA fluorescence of residual parathyroid (C & D) [100] (Reproduced from Ref. [100] with permission. Copyright 2019 Elsevier Ltd). (For interpretation of the references to colour in this figure legend, the reader is referred to the Web version of this article.)

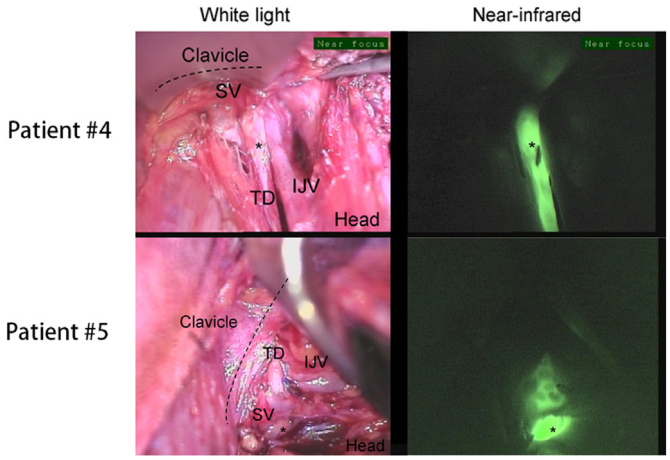

Fig. 10. NIR imaging of thoracic ducts for patients #4 and #5 [109]. (IJV: internal jugular vein; SV: subclavian vein; TD: thoracic duct) (Reproduced from Ref. [109] with permission. Copyright 2018, Society of Surgical Oncology).

NIR-FI, a great deal of surgical dissection work is required before FI can be visualized optimally, which inevitably prolongs the procedure time.

5. Challenges

We believe that OI diagnosis and treatment will have a broad application prospect in TC, but the exploration of clinical translation has also revealed unavoidable shortcomings. In the diagnosis and treatment of thyroid nodules, fluorescence imaging can only obtain two-dimensional image information of the tumor; OCT is only suitable for surgeons to explore the area of interest during surgery because the imaging depth is limited to 1–2 mm; PAI is easily affected by motion artifacts, thus reducing the image quality; DOT imaging is more time-consuming, and there is still a lack of relevant studies in the field of thyroid. The limited depth of penetration has become the biggest obstacle to the clinical translation of OI. How to avoid the influence of optical properties (scattering, refraction and absorption) on the stability of imaging and ensure the quality of imaging has also become an urgent problem to be addressed. In addition, NIR-II fluorescence imaging, as the most promising imaging modality in OI, still has a long way to go for its clinical translation. The ideal fluorescent probe should have long fluorescence emission time, good photostability and water solubility, non-toxic or low toxicity, easy metabolism, high quantum yield, and tumor-specific enrichment. To date, only three NIR fluorescent probes have been authorized by the FDA for clinical use: ICG, methylene blue, and 5-ALA. More outstanding targeted fluorescent probes remain to be explored. The specific advantages and disadvantages of the four imaging modalities are clearly shown in Table 4. In the last decade, researchers have explored the utility of OI and therapy in the diagnosis and treatment of TC, but there is a lack of unified parametric standards for OI (e.g., in the assessment of fluorescence signal intensity and quantification time [83]), and no consensus on a system for evaluating the effectiveness of optical therapy. Also, advanced and standardized OI cameras need to be improved and developed. In addition, a large amount of research on optical diagnosis and treatment of TC are still in stages of basic research, and clinical data are relatively lacking. There is still a lot of work to be done in the process of OI to clinical translation.

Concerning optical therapy, we believe that it is still underdeveloped compared to conventional treatments for TC and its clinical translation is still very challenging. DTC, which accounts for more than 95% of TCs, is generally treated by surgical resection (open surgery or lumpectomy), which is economical and has an excellent prognosis. In addition to the advantages of non-invasive nature of optical thermal therapy, other aspects, such as long-term toxic effects and prognostic follow-up, are still blank. The need for OI to ensure the same or even higher treatment efficiency as surgical treatment while controlling medical costs will be a very big challenge. However, for ATC, which is highly malignant, the clinical application of optical therapy has been most significant in improving the quality of survival, prolonging the survival period, and even curing the cancer.

6. Conclusions and further perspectives

Despite the aforementioned drawbacks of OI, it is undeniable that overdiagnosis of thyroid nodules is widespread and there is an urgent need for new and more accurate diagnostic and treatment modalities to be added to reduce the cost of treatment. The diagnosis of thyroid nodules by conventional ultrasound relies on image quality, neck coverage area and interpretation by the diagnostic ultrasonographic. The current gold standard for confirming the diagnosis of TC is FNAB, but it still has a high probability of failing to characterize thyroid nodules as an invasive diagnostic method with minimal coverage area. These may be the reasons for over-treatment of thyroid nodules. The great advantage of OI is that it is highly safe and at the same time highly malleable. The superior multi-modality diagnostic platform needs to be further explored and the

Table 4
The specific advantages and disadvantages of the four imaging modalities.

	NIR-II FI	OCT	PAI	DOT
Common Advantages	1. Non-invasive 2. High biocompatibility 3. No radiation 4. High resolution 5. No barriers to multimodal treatment combination 6. Accurate characterization and localization			
Common Disadvantages	1. Relatively poor depth compared to PET, MRI, or X-ray based techniques 2. Unstable image quality due to optical limitations and thyroid gland structure near the trachea			
Unique Advantages	1. Flexible modifiability for targeted imaging 2. Precise data for clinical staging 3. Real-time feedback for surgical navigation	1. Convenient, short imaging time 2. Real-time feedback for surgical navigation	1. Detects small vessels that are not detected by color Doppler ultrasound 2. Displays key functional data (e.g., oxygen saturation)	1. Three-dimensional imaging 2. Imaging of thick tissue bodies
Unique Disadvantages	1. Strong background signal of tumor tissue with increased vascularity may interfere with the imaging of FI 2. Two-dimensional imaging	1. OCT has the most limited penetration depth (1–2 mm) and intraoperative thyroid imaging is limited to the exposed surface and superficial tissues to be performed.	1. Susceptible to motion artifacts and difficult to control image quality	1. Long imaging time
Penetration Depth	Near NIR-II laser depth up to 5–20 mm	500 μm-2 mm	Penetration depth and resolution are inversely proportional to the frequency of the ultrasound detector used (center frequency of 4–6 MHz and a bandwidth of 0.1–10 MHz for an imaging depth of 2–4 cm)	1–1.5 cm

advantages complement each other, which is very promising to achieve accurate qualitative and localized diagnosis of thyroid nodules. The superiority of OI lies not only in the non-invasive nature, high safety, and diagnostic specificity, but also in the excellent performance of phototherapy in facilitating TC treatment. The clinical translation of phototherapy is mainly limited by the depth of penetration, Qiaolin Li et al. proposed the first minimally invasive laparoscopic photothermal ablation (L-A PTA) method [110], which opened a new avenue for optical treatment of deep tumors. Although the clinical translation of optical therapy in the field of TC treatment is currently proceeding quite slowly, researches on the application of optical imaging surgical navigation in clinical practice have progressed by leaps and bounds. In particular, FI has been clinically explored extensively, and it has proven to be beneficial for the complete clearance of TCs and their metastatic lymph nodes to tremendously reduce the incidence of parathyroid, nerve, vascular, and thoracic duct injuries. Fluorescent probes have shown excellent flexibility in chemical modification, which not only can build targeted tumor imaging, precision nano-delivery, and surgical navigation on a single platform, but also can capture the optical properties of certain materials to achieve non-invasive precision treatment of tumors in combination with PDT or PTT. This is of great significance for the treatment of ACT with high malignancy.

In addition, a novel cancer therapy called near-infrared photoimmunotherapy (NIR-PIT) was developed in the trend of photothermal and photochemotherapy to directly kill cancer cells while generating an immune response in the host [111]. NIR-PIT consists of near-infrared light irradiation, fluorescent dyes, and tumor-targeting antibodies [112] (e.g., EGFR antibodies for head and neck cancers). Local irradiation can stimulate ligand release and improve the targeting of immunotherapy.FI can follow the metabolic distribution of drugs in vivo to assess prognosis. We firmly believe that NIR-PIT is a very promising therapeutic approach in the field of TC treatment, especially in the most malignant undifferentiated cancers, but relevant studies are still vacant and need to be further explored by researchers.

A growing number of studies have documented the critical role that OI plays in the diagnosis and treatment of TC. OI can not only improve the correct diagnosis of thyroid nodules and reduce the operational cost of invasive examinations, but can also be applied to the treatment of TC in various forms, such as PTT, PDT, construction of light-activated nanodelivery platforms, and surgical navigation. OI is a promising and potential alternative to conventional TC screening programs. Optical therapy has shown excellent controllability and high efficiency in killing tumor cells. OI, in combination with other treatment modalities, can build superior multifunctional nano-diagnostic treatment platforms. We trust that multimodal nano-optical diagnostic and therapeutic platforms will become a trend in cancer treatment and diagnosis and will successfully move towards clinical practice applications in the near future.

7. Funding

This work was supported by Zhejiang Provincial Natural Science Foundation [grant number LY21H160049] and Traditional Chinese medicine science and technology projects in Zhejiang Province [grant number 2022ZB020].

Declaration of competing interest

The authors declare that they have no known competing financial interests or personal relationships that could have appeared to influence the work reported in this paper.

Data availability

No data was used for the research described in the article.

References

[1] H. Qiu, S. Cao, R. Xu, Cancer incidence, mortality, and burden in China: a time-trend analysis and comparison with the United States and United Kingdom based on the global epidemiological data released in 2020, Cancer Commun. 41 (10) (2021) 1037–1048, https://doi.org/10.1002/cac2.12197.

[2] B.A. Kilfoy, T. Zheng, T.R. Holford, X. Han, M.H. Ward, A. Sjodin, Y. Zhang, Y. Bai, C. Zhu, G.L. Guo, N. Rothman, Y. Zhang, International patterns and trends in thyroid cancer incidence, 1973–2002, Cancer Cause, Control 20 (5) (2009) 525–531, https://doi.org/10.1007/s10552-008-9260-4.

[3] L. Davies, H.G. Welch, Current thyroid cancer trends in the United States, JAMA Otolaryngol. Head Neck Surgery 140 (4) (2014) 317–322, https://doi.org/10.1001/jamaoto.2014.1.

[4] S. Vaccarella, S. Franceschi, F. Bray, C.P. Wild, M. Plummer, L. Dal Maso, Worldwide thyroid-cancer epidemic? The increasing impact of overdiagnosis, N. Engl. J. Med. 375 (7) (2016) 614–617, https://doi.org/10.1056/NEJMp1604412.

[5] D.S. Cooper, G.M. Doherty, B.R. Haugen, R.T. Kloos, S.L. Lee, S.J. Mandel, E.L. Mazzaferri, B. McIver, F. Pacini, M. Schlumberger, S.I. Sherman, D.L. Steward, R.M. Tuttle, Revised American thyroid association management guidelines for patients with thyroid nodules and differentiated thyroid cancer, Thyroid 19 (11) (2009) 1167–1214, https://doi.org/10.1089/thy.2009.0110.

[6] B.R. Haugen, E.K. Alexander, K.C. Bible, G.M. Doherty, S.J. Mandel, Y.E. Nikiforov, F. Pacini, G.W. Randolph, A.M. Sawka, M. Schlumberger, K.G. Schuff, S.I. Sherman, J.A. Sosa, D.L. Steward, R.M. Tuttle, L. Wartofsky, 2015 American thyroid association management guidelines for adult patients with thyroid nodules and differentiated thyroid cancer: the American thyroid association guidelines task force on thyroid nodules and differentiated thyroid cancer, Thyroid 26 (1) (2016) 1–133, https://doi.org/10.1089/thy.2015.0020.

[7] S. Filetti, C. Durante, D. Hartl, S. Leboulleux, L.D. Locati, K. Newbold, M.G. Papotti, A. Berruti, Thyroid cancer: ESMO Clinical Practice Guidelines for diagnosis, treatment and follow-up, Ann. Oncol. 30 (12) (2019) 1856–1883, https://doi.org/10.1093/annonc/mdz400.

[8] H. Lim, S.S. Devesa, J.A. Sosa, D. Check, C.M. Kitahara, Trends in thyroid cancer incidence and mortality in the United States, 1974-2013, JAMA 317 (13) (2017) 1338, https://doi.org/10.1001/jama.2017.2719.

[9] N. Prasongsook, A. Kumar, A.V. Chintakuntlawar, R.L. Foote, J. Kasperbauer, J. Molina, Y. Garces, D. Ma, M.A.N. Wittich, J. Rubin, R. Richardson, J. Morris, I. Hay, V. Fatourechi, B. McIver, M. Ryder, G. Thompson, C. Grant, M. Richards, T.J. Sebo, M. Rivera, V. Suman, S.M. Jenkins, R.C. Smallridge, K.C. Bible, Survival in response to multimodal therapy in anaplastic thyroid cancer, J. Clin. Endocrinol. Metab. 102 (12) (2017) 4506–4514, https://doi.org/10.1210/jc.2017-01180.

[10] K.C. Bible, E. Kebebew, J. Brierley, J.P. Brito, M.E. Cabanillas, T.J. Clark, A. Di Cristofano, R. Foote, T. Giordano, J. Kasperbauer, K. Newbold, Y.E. Nikiforov, G. Randolph, M.S. Rosenthal, A.M. Sawka, M. Shah, A. Shaha, R. Smallridge, C.K. Wong-Clark, 2021 American thyroid association guidelines for management of patients with anaplastic thyroid cancer, Thyroid 31 (3) (2021) 337–386, https://doi.org/10.1089/thy.2020.0944.

[11] E. Chahardahmasumi, R. Salehidoost, M. Amini, A. Aminorroaya, H. Rezvanian, A. Kachooei, B. Iraj, M. Nazem, M. Kolahdoozan, Assessment of the early and late complication after thyroidectomy, Adv. Biomed. Res. 8 (1) (2019) 14, https://doi.org/10.4103/abr.abr_3_19.

[12] M.H. Niemz, Laser-tissue interactions: fundamentals and applications, Adv. Biol. Med. Phys. 36 (3) (2007) 216–220, https://doi.org/10.1007/978-3-662-03193-3.

[13] I. Fatima, A. Rahdar, S. Sargazi, M. Barani, M. Hassanisaadi, V.K. Thakur, Quantum dots: synthesis, antibody conjugation, and HER2-receptor targeting for breast cancer therapy, J. Funct. Biomater. 12 (4) (2021) 75, https://doi.org/10.3390/jfb12040075.

[14] Q. Yu, S. Huang, Z. Wu, J. Zheng, X. Chen, L. Nie, Label-free visualization of early cancer hepatic micrometastasis and intraoperative image-guided surgery by photoacoustic imaging, J. Nucl. Med. 61 (7) (2020) 1079–1085, https://doi.org/10.2967/jnumed.119.233155.

[15] M. Barani, M. Zeeshan, D. Kalantar-Neyestanaki, M.A. Farooq, A. Rahdar, N.K. Jha, S. Sargazi, P.K. Gupta, V.K. Thakur, Nanomaterials in the management of gram-negative bacterial infections, Nanomaterials 11 (10) (2021) 2535, https://doi.org/10.3390/nano11102535.

[16] M. Barani, S. Sargazi, V. Mohammadzadeh, A. Rahdar, S. Pandey, N.K. Jha, P.K. Gupta, V.K. Thakur, Theranostic advances of bionanomaterials against gestational diabetes mellitus: a preliminary review, J. Funct. Biomater. 12 (4) (2021) 54, https://doi.org/10.3390/jfb12040054.

[17] K. Rizwan, A. Rahdar, M. Bilal, H.M.N. Iqbal, MXene-based electrochemical and biosensing platforms to detect toxic elements and pesticides pollutants from environmental matrices, Chemosphere 291 (Pt 1) (2022), 132820, https://doi.org/10.1016/j.chemosphere.2021.132820.

[18] J. Najeeb, U. Farwa, F. Ishaque, H. Munir, A. Rahdar, M.F. Nazar, M.N. Zafar, Surfactant stabilized gold nanomaterials for environmental sensing applications – a review, Environ. Res. 208 (2022), 112644, https://doi.org/10.1016/j.envres.2021.112644.

[19] M. Batool, M.F. Nazar, A. Awan, M.B. Tahir, A. Rahdar, A.E. Shalan, S. Lanceros-Méndez, M.N. Zafar, Bismuth-based heterojunction nanocomposites for photocatalysis and heavy metal detection applications, Nano-Struct. Nano-Objects 27 (2021), 100762, https://doi.org/10.1016/j.nanoso.2021.100762.

[20] P.N. Prasad, B.R. Masters, Introduction to biophotonics, J. Biomed. Opt. 10 (3) (2005), 039901, https://doi.org/10.1117/1.1931672.

[21] S. Sargazi, I. Fatima, M. Hassan Kiani, V. Mohammadzadeh, R. Arshad, M. Bilal, A. Rahdar, A.M. Díez-Pascual, R. Behzadmehr, Fluorescent-based nanosensors for selective detection of a wide range of biological macromolecules: a comprehensive review, Int. J. Biol. Macromol. 206 (2022) 115–147, https://doi.org/10.1016/j.ijbiomac.2022.02.137.

[22] R.Q. Yang, K.L. Lou, P.Y. Wang, Y.Y. Gao, Y.Q. Zhang, M. Chen, W.H. Huang, G.J. Zhang, Surgical navigation for malignancies guided by near-infrared-II fluorescence imaging, Small Methods 5 (3) (2021), 2001066, https://doi.org/10.1002/smtd.202001066.

[23] Z. Feng, T. Tang, T. Wu, X. Yu, Y. Zhang, M. Wang, J. Zheng, Y. Ying, S. Chen, J. Zhou, X. Fan, D. Zhang, S. Li, M. Zhang, J. Qian, Perfecting and extending the near-infrared imaging window, Light Sci. Appl. 10 (1) (2021) 197, https://doi.org/10.1038/s41377-021-00628-0.

[24] Z. Luo, D. Hu, D. Gao, Z. Yi, H. Zheng, Z. Sheng, X. Liu, High-specificity in vivo tumor imaging using bioorthogonal NIR-IIb nanoparticles, Adv. Mater. 33 (49) (2021), 2102950, https://doi.org/10.1002/adma.202102950.

[25] K. Cheng, H. Chen, C.H. Jenkins, G. Zhang, W. Zhao, Z. Zhang, F. Han, J. Fung, M. Yang, Y. Jiang, L. Xing, Z. Cheng, Synthesis, characterization, and biomedical applications of a targeted dual-modal near-infrared-II fluorescence and photoacoustic imaging nanoprobe, ACS Nano 11 (12) (2017) 12276–12291, https://doi.org/10.1021/acsnano.7b05966.

[26] X. Chen, H. Zhu, X. Huang, P. Wang, F. Zhang, W. Li, G. Chen, B. Chen, Novel iodinated gold nanoclusters for precise diagnosis of thyroid cancer, Nanoscale 9 (6) (2017) 2219–2231, https://doi.org/10.1039/C6NR07656D.

[27] D. Fanfone, D. Stanicki, D. Nonclercq, M. Port, L. Vander Elst, S. Laurent, R.N. Muller, S. Saussez, C. Burtea, Molecular imaging of galectin-1 expression as a biomarker of papillary thyroid cancer by using peptide-functionalized imaging probes, Biology 9 (3) (2020) 53, https://doi.org/10.3390/biology9030053.

[28] L. Cortese, G. Lo Presti, M. Zanoletti, G. Aranda, M. Buttafava, D. Contini, A. Dalla Mora, H. Dehghani, L. Di Sieno, S. de Fraguier, F.A. Hanzu, M. Mora Porta, A. Nguyen-Dinh, M. Renna, B. Rosinski, M. Squarcia, A. Tosi, U.M. Weigel, S. Wojtkiewicz, T. Durduran, The LUCA device: a multi-modal platform combining diffuse optics and ultrasound imaging for thyroid cancer screening, Biomed. Opt Express 12 (6) (2021) 3392, https://doi.org/10.1364/BOE.416561.

[29] C.M. Weekley, H.H. Harris, Which form is that? The importance of selenium speciation and metabolism in the prevention and treatment of disease, Chem. Soc. Rev. 42 (23) (2013) 8870, https://doi.org/10.1039/c3cs60272a.

[30] K.M. Brown, J.R. Arthur, Selenium, selenoproteins and human health: a review, Publ. Health Nutr. 4 (2b) (2001) 593–599, https://doi.org/10.1079/PHN2001143.

[31] G.V. Kryukov, S. Castellano, S.V. Novoselov, A.V. Lobanov, O. Zehtab, R. Guigó, V.N. Gladyshev, Characterization of mammalian selenoproteomes, Science 300 (5624) (2003) 1439–1443, https://doi.org/10.1126/science.1083516.

[32] X. Luo, R. Wang, C. Lv, G. Chen, J. You, F. Yu, Detection of selenocysteine with a ratiometric near-infrared fluorescent probe in cells and in mice thyroid diseases model, Anal. Chem. 92 (1) (2020) 1589–1597, https://doi.org/10.1021/acs.analchem.9b04860.

[33] U. Laraib, S. Sargazi, A. Rahdar, M. Khatami, S. Pandey, Nanotechnology-based approaches for effective detection of tumor markers: a comprehensive state-of-the-art review, Int. J. Biol. Macromol. 195 (2022) 356–383, https://doi.org/10.1016/j.ijbiomac.2021.12.052.

[34] M. Mukhtar, S. Sargazi, M. Barani, H. Madry, A. Rahdar, M. Cucchiarini, Application of nanotechnology for sensitive detection of low-abundance single-nucleotide variations in genomic DNA: a review, Nanomaterials 11 (6) (2021) 1384, https://doi.org/10.3390/nano11061384.

[35] C. Zhou, Y. Wang, A.D. Aguirre, T. Tsai, D.W. Cohen, J.L. Connolly, J.G. Fujimoto, Ex vivo imaging of human thyroid pathology using integrated optical coherence tomography and optical coherence microscopy, J. Biomed. Opt. 15 (1) (2010), 016001, https://doi.org/10.1117/1.3306696.

[36] H.S. Lee, S.W. Shin, J.K. Bae, W.G. Jung, S.W. Kim, C. Oak, B.K. Chun, Y. Ahn, B. Lee, K.D. Lee, Preliminary study of optical coherence tomography imaging to identify microscopic extrathyroidal extension in patients with papillary thyroid carcinoma, Laser Surg. Med. 48 (4) (2016) 371–376, https://doi.org/10.1002/lsm.22466.

[37] N. Yang, C. Boudoux, E. De Montigny, A. Maniakas, O. Gologan, W.J. Madore, S. Khullar, L. Guertin, A. Christopoulos, E. Bissada, T. Ayad, Rapid head and neck tissue identification in thyroid and parathyroid surgery using optical coherence tomography, Head Neck 41 (12) (2019) 4171–4180, https://doi.org/10.1002/hed.25972.

[38] A. Karlas, M.A. Pleitez, J. Aguirre, V. Ntziachristos, Optoacoustic imaging in endocrinology and metabolism, Nat. Rev. Endocrinol. 17 (6) (2021) 323–335, https://doi.org/10.1038/s41574-021-00482-5.

[39] J. Lv, Y. Xu, L. Xu, L. Nie, Quantitative functional evaluation of liver fibrosis in mice with dynamic contrast-enhanced photoacoustic imaging, Radiology 300 (1) (2021) 89–97, https://doi.org/10.1148/radiol.2021204134.

[40] A. Dima, V. Ntziachristos, In-vivo handheld optoacoustic tomography of the human thyroid, Photoacoustics 4 (2) (2016) 65–69, https://doi.org/10.1016/j.pacs.2016.05.003.

[41] V.S. Dogra, B.K. Chinni, K.S. Valluru, J. Moalem, E.J. Giampoli, K. Evans, N.A. Rao, Preliminary results of ex vivo multispectral photoacoustic imaging in the management of thyroid cancer, Am. J. Roentgenol. 202 (6) (2014) W552–W558, https://doi.org/10.2214/AJR.13.11433.

[42] M. Yang, L. Zhao, X. He, N. Su, C. Zhao, H. Tang, T. Hong, W. Li, F. Yang, L. Lin, B. Zhang, R. Zhang, Y. Jiang, C. Li, Photoacoustic/ultrasound dual imaging of human thyroid cancers: an initial clinical study, Biomed. Opt Express 8 (7) (2017) 3449, https://doi.org/10.1364/BOE.8.003449.

[43] W. Roll, N.A. Markwardt, M. Masthoff, A. Helfen, J. Claussen, M. Eisenblätter, A. Hasenbach, S. Hermann, A. Karlas, M. Wildgruber, V. Ntziachristos, M. Schäfers, Multispectral optoacoustic tomography of benign and malignant thyroid disorders: a pilot study, J. Nucl. Med. 60 (10) (2019) 1461–1466, https://doi.org/10.2967/jnumed.118.222174.

[44] J. Kim, E. Park, B. Park, W. Choi, K.J. Lee, C. Kim, Towards clinical photoacoustic and ultrasound imaging: probe improvement and real-time graphical user interface, Exp. Biol. Med. 245 (4) (2020) 321–329, https://doi.org/10.1177/1535370219889968.

[45] J. Zouaoui, L. Di Sieno, L. Hervé, A. Pifferi, A. Farina, A.D. Mora, J. Derouard, J. Dinten, Chromophore decomposition in multispectral time-resolved diffuse optical tomography, Biomed. Opt Express 8 (10) (2017) 4772, https://doi.org/10.1364/BOE.8.004772.

[46] T. Shimokawa, T. Ishii, Y. Takahashi, S. Sugawara, M. Sato, O. Yamashita, Diffuse optical tomography using multi-directional sources and detectors, Biomed. Opt Express 7 (7) (2016) 2623, https://doi.org/10.1364/BOE.7.002623.

[47] T. Mimura, S. Okawa, H. Kawaguchi, Y. Tanikawa, Y. Hoshi, Imaging the human thyroid using three-dimensional diffuse optical tomography: a preliminary study, Appl. Sci. 11 (4) (2021) 1670, https://doi.org/10.3390/app11041670.

[48] H. Fujii, Y. Yamada, K. Kobayashi, M. Watanabe, Y. Hoshi, Modeling of light propagation in the human neck for diagnoses of thyroid cancers by diffuse optical tomography, Int. J. Numer. Meth. Bio. 33 (5) (2017), e2826, https://doi.org/10.1002/cnm.2826.

[49] R. Biswas, P. Chung, J.H. Moon, S. Lee, J. Ahn, Carboplatin synergistically triggers the efficacy of photodynamic therapy via caspase 3-, 8-, and 12-dependent pathways in human anaplastic thyroid cancer cells, Laser Med. Sci. 29 (3) (2014) 995–1007, https://doi.org/10.1007/s10103-013-1452-9.

[50] S. Begum, E. Rosenbaum, R. Henrique, Y. Cohen, D. Sidransky, W.H. Westra, BRAF mutations in anaplastic thyroid carcinoma: implications for tumor origin, diagnosis and treatment, Mod. Pathol. 17 (11) (2004) 1359–1363, https://doi.org/10.1038/modpathol.3800198.

[51] X. Li, J.F. Lovell, J. Yoon, X. Chen, Clinical development and potential of photothermal and photodynamic therapies for cancer, Nat. Rev. Clin. Oncol. 17 (11) (2020) 657–674, https://doi.org/10.1038/s41571-020-0410-2.

[52] Q. Wang, G. Sui, X. Wu, D. Teng, L. Zhu, S. Guan, H. Ran, Z. Wang, H. Wang, A sequential targeting nanoplatform for anaplastic thyroid carcinoma theranostics, Acta Biomater. 102 (2020) 367–383, https://doi.org/10.1016/j.actbio.2019.11.043.

[53] S. Huang, Y. Wu, C. Li, L. Xu, J. Huang, Y. Huang, W. Cheng, B. Xue, L. Zhang, S. Liang, X. Jin, X. Zhu, S. Xiong, Y. Su, H. Wang, Tailoring morphologies of mesoporous polydopamine nanoparticles to deliver high-loading radioiodine for anaplastic thyroid carcinoma imaging and therapy, Nanoscale 13 (35) (2021) 15021–15030, https://doi.org/10.1039/D1NR02892H.

[54] C. Zhang, J. Chai, Q. Jia, J. Tan, Z. Meng, N. Li, M. Yuan, Evaluating the therapeutic efficacy of radiolabeled BSA@CuS nanoparticle-induced radio-photothermal therapy against anaplastic thyroid cancer, IUBMB Life 74 (5) (2022) 433–445, https://doi.org/10.1002/iub.2601.

[55] X. Xing, K. Yang, B. Li, S. Tan, J. Yi, X. Li, E. Pang, B. Wang, X. Song, M. Lan, Boron dipyrromethene-based phototheranostics for near infrared fluorescent and photoacoustic imaging-guided synchronous photodynamic and photothermal therapy of cancer, J. Phys. Chem. Lett. 13 (34) (2022) 7939–7946, https://doi.org/10.1021/acs.jpclett.2c02122.

[56] M. Xu, D. Zhao, Y. Chen, C. Chen, L. Zhang, L. Sun, J. Chen, Q. Tang, S. Sun, C. Ma, X. Liang, S. Wang, Charge reversal polypyrrole nanocomplex-mediated gene delivery and photothermal therapy for effectively treating papillary thyroid cancer and inhibiting lymphatic metastasis, ACS Appl. Mater. Interfaces 14 (12) (2022) 14072–14086, https://doi.org/10.1021/acsami.1c25179.

[57] M. Amaral, A.J. Charmier, R.A. Afonso, J. Catarino, P. Faísca, L. Carvalho, L. Ascensão, J.M.P. Coelho, M.M. Gaspar, C.P. Reis, Gold-based nanoplataform for the treatment of anaplastic thyroid carcinoma: a step forward, Cancers 13 (6) (2021) 1242, https://doi.org/10.3390/cancers13061242.

[58] T. Yu, L. Tong, Y. Ao, G. Zhang, Y. Liu, H. Zhang, Novel design of NIR-triggered plasmonic nanodots capped mesoporous silica nanoparticles loaded with natural capsaicin to inhibition of metastasis of human papillary thyroid carcinoma B-CPAP cells in thyroid cancer chemo-photothermal therapy, J. Photochem. Photobiol. B Biol. 197 (2019), 111534, https://doi.org/10.1016/j.jphotobiol.2019.111534.

[59] Y. Tan, P. Liu, D. Li, D. Wang, B.Z. Tang, NIR-II aggregation-induced emission luminogens for tumor phototheranostics, Biosensors 12 (1) (2022) 46, https://doi.org/10.3390/bios12010046.

[60] P. Zhao, Z. Jin, Q. Chen, T. Yang, D. Chen, J. Meng, X. Lu, Z. Gu, Q. He, Local generation of hydrogen for enhanced photothermal therapy, Nat. Commun. 9 (1) (2018) 4241, https://doi.org/10.1038/s41467-018-06630-2.

[61] G. Zhou, Y.S. Wang, Z. Jin, P. Zhao, H. Zhang, Y. Wen, Q. He, Porphyrin–palladium hydride MOF nanoparticles for tumor-targeting photoacoustic imaging-guided hydrogenothermal cancer therapy, Nanoscale Horizons 4 (5) (2019) 1185–1193, https://doi.org/10.1039/C9NH00021F.

[62] L.G. Fedyniak, Photodynamic therapy for cancer, Posit. Health 50 (6827) (2005) 589–590, https://doi.org/10.1136/gut.50.4.549.

[63] Z. Yu, Q. Sun, W. Pan, N. Li, B. Tang, A near-infrared triggered nanophotosensitizer inducing domino effect on mitochondrial reactive oxygen species burst for cancer therapy, ACS Nano 9 (11) (2015) 11064–11074, https://doi.org/10.1021/acsnano.5b04501.

[64] D. Sheng, T. Liu, L. Deng, L. Zhang, X. Li, J. Xu, L. Hao, P. Li, H. Ran, H. Chen, Perfluorooctyl bromide & indocyanine green co-loaded nanoliposomes for enhanced multimodal imaging-guided phototherapy, Biomaterials 1 (2018), https://doi.org/10.1016/j.biomaterials.2018.02.041.

[65] X. Song, L. Feng, C. Liang, K. Yang, Z. Liu, Ultrasound triggered tumor oxygenation with oxygen-shuttle nanoperfluorocarbon to overcome hypoxia-associated resistance in cancer therapies, Nano Lett. 16 (10) (2016) 6145–6153, https://doi.org/10.1021/acs.nanolett.6b02365.

[66] S. Phua, G. Yang, Q.L. Wei, A. Verma, Y. Zhao, Catalase integrated hyaluronic acid as nanocarriers for enhanced photodynamic therapy in solid tumor, ACS Nano 13 (4) (2019), https://doi.org/10.1021/acsnano.9b01087.

[67] H. Chen, J. Tian, W. He, Z. Guo, H2O2 activatable and O2-evolving nanoparticles for highly efficient and selective photodynamic therapy against hypoxic tumor cells, J. Am. Chem. Soc. 137 (4) (2015) 1539–1547, https://doi.org/10.1021/ja511420n.

[68] N. Muhanna, H.H.L. Chan, J.L. Townson, C.S. Jin, L. Ding, M.S. Valic, C.M. Douglas, C.M. MacLaughlin, J. Chen, G. Zheng, J.C. Irish, Photodynamic therapy enables tumor-specific ablation in preclinical models of thyroid cancer, Endocr. Relat. Cancer 27 (2) (2020) 41–53, https://doi.org/10.1530/ERC-19-0258.

[69] S. Chatterjee, Y. Rhee, P. Chung, R. Ge, J. Ahn, Sulforaphene enhances the efficacy of photodynamic therapy in anaplastic thyroid cancer through ras/RAF/MEK/ERK pathway suppression, J. Photochem. Photobiol. B Biol. 179 (2018) 46–53, https://doi.org/10.1016/j.jphotobiol.2017.12.013.

[70] R. Biswas, A. Mondal, J. Ahn, Deregulation of EGFR/PI3K and activation of PTEN by photodynamic therapy combined with carboplatin in human anaplastic thyroid cancer cells and xenograft tumors in nude mice, J. Photochem. Photobiol., B 148 (2015) 118–127, https://doi.org/10.1016/j.jphotobiol.2015.03.024.

[71] H. Kim, S.W. Kim, K.H. Seok, C.W. Hwang, J. Ahn, J. Jin, H.W. Kang, Hypericin-assisted photodynamic therapy against anaplastic thyroid cancer, Photodiagn. Photodyn. 24 (2018) 15–21, https://doi.org/10.1016/j.pdpdt.2018.08.008.

[72] D. Yan, W. Xie, J. Zhang, L. Wang, D. Wang, B.Z. Tang, Donor/π-Bridge manipulation for constructing a stable NIR-II aggregation-induced emission luminogen with balanced phototheranostic performance, Angew. Chem. 60 (51) (2021) 26769–26776, https://doi.org/10.1002/anie.202111767.

[73] Y. Dai, H. Zhao, K. He, W. Du, Y. Kong, Z. Wang, M. Li, Q. Shen, P. Sun, Q. Fan, NIR-II excitation phototheranostic nanomedicine for fluorescence/photoacoustic tumor imaging and targeted photothermal-photonic thermodynamic therapy, Small 17 (42) (2021), 2102527, https://doi.org/10.1002/smll.202102527.

[74] Q. Wang, Y. Ji, J. Shi, L. Wang, NIR-driven water splitting H 2 production nanoplatform for H 2 -mediated cascade-amplifying synergetic cancer therapy, ACS Appl. Mater. Interfaces 12 (21) (2020) 23677–23688, https://doi.org/10.1021/acsami.0c03852.

[75] B. Schmidbauer, K. Menhart, D. Hellwig, J. Grosse, Differentiated thyroid cancer—treatment: state of the art, Int. J. Mol. Sci. 18 (6) (2017) 1292, https://doi.org/10.3390/ijms18061292.

[76] E.J. Sherman, S.H. Lim, A.L. Ho, R.A. Ghossein, M.G. Fury, A.R. Shaha, M. Rivera, O. Lin, S. Wolden, N.Y. Lee, D.G. Pfister, Concurrent doxorubicin and radiotherapy for anaplastic thyroid cancer: a critical re-evaluation including uniform pathologic review, Radiother. Oncol. 101 (3) (2011) 425–430, https://doi.org/10.1016/j.radonc.2011.09.004.

[77] M. Zhou, Y. Chen, M. Adachi, X. Wen, B. Erwin, O. Mawlawi, S.Y. Lai, C. Li, Single agent nanoparticle for radiotherapy and radio-photothermal therapy in anaplastic thyroid cancer, Biomaterials 57 (2015) 41–49, https://doi.org/10.1016/j.biomaterials.2015.04.013.

[78] R.C. Smallridge, K.B. Ain, S.L. Asa, K.C. Bible, J.D. Brierley, K.D. Burman, E. Kebebew, N.Y. Lee, Y.E. Nikiforov, M.S. Rosenthal, M.H. Shah, A.R. Shaha, R.M. Tuttle, American Thyroid Association guidelines for management of patients with anaplastic thyroid cancer, Thyroid : official journal of the American Thyroid Association. 22 (11) (2012) 1104–1139, https://doi.org/10.1089/thy.2012.0302.

[79] T. Yu, L. Tong, Y. Ao, G. Zhang, Y. Liu, H. Zhang, NIR triggered PLGA coated Au-TiO(2) core loaded CPT-11 nanoparticles for human, Drug Deliv. 27 (1) (2020) 855–863, https://doi.org/10.1080/10717544.2020.1775723.

[80] R. Arshad, I. Fatima, S. Sargazi, A. Rahdar, M. Karamzadeh-Jahromi, S. Pandey, A.M. Díez-Pascual, M. Bilal, Novel perspectives towards RNA-based nano-theranostic approaches for cancer management, Nanomaterials 11 (12) (2021) 3330, https://doi.org/10.3390/nano11123330.

[81] Y. Liu, V. Gunda, X. Zhu, X. Xu, J. Wu, D. Askhatova, O.C. Farokhzad, S. Parangi, J. Shi, Theranostic near-infrared fluorescent nanoplatform for imaging and systemic siRNA delivery to metastatic anaplastic thyroid cancer, Proc. Natl. Acad. Sci. USA 113 (28) (2016) 7750–7755, https://doi.org/10.1073/pnas.1605841113.

[82] S. Sargazi, M. Mukhtar, A. Rahdar, M. Bilal, M. Barani, A.M. Díez-Pascual, R. Behzadmehr, S. Pandey, Opportunities and challenges of using high-sensitivity nanobiosensors to detect long noncoding RNAs: a preliminary review, Int. J. Biol. Macromol. 205 (2022) 304–315, https://doi.org/10.1016/j.ijbiomac.2022.02.082.

[83] C. Wang, Z. Wang, T. Zhao, Y. Li, G. Huang, B.D. Sumer, J. Gao, Optical molecular imaging for tumor detection and image-guided surgery, Biomaterials 157 (2018) 62–75, https://doi.org/10.1016/j.biomaterials.2017.12.002.

[84] A.M. Smith, M.C. Mancini, S. Nie, Bioimaging: second window for in vivo imaging, Nat. Nanotechnol. 4 (11) (2009) 710–711, https://doi.org/10.1038/nnano.2009.326.

[85] Kenry, Yukun, Duan, Bin, Liu, Biological imaging: recent advances of optical imaging in the second near-infrared window (adv. Mater. 47/2018), Adv. Mater. 30 (47) (2017) 1870361, https://doi.org/10.1002/adma.201870361, 1870361.

[86] T. Namikawa, Clinical applications of 5-aminolevulinic acid-mediated fluorescence for gastric cancer, World J. Gastroenterol. 21 (29) (2015) 8769, https://doi.org/10.3748/wjg.v21.i29.8769.
[87] A. Matsui, E. Tanaka, H.S. Choi, V. Kianzad, S. Gioux, S.J. Lomnes, J.V. Frangioni, Real-time, near-infrared, fluorescence-guided identification of the ureters using methylene blue, Surgery 148 (1) (2010) 78–86, https://doi.org/10.1016/j.surg.2009.12.003.
[88] L. van Manen, H.J.M. Handgraaf, M. Diana, J. Dijkstra, T. Ishizawa, A.L. Vahrmeijer, J.S.D. Mieog, A practical guide for the use of indocyanine green and methylene blue in fluorescence-guided abdominal surgery, J. Surg. Oncol. 118 (2) (2018) 283–300, https://doi.org/10.1002/jso.25105.
[89] K. Büther, M.G. Compeer, J.G.R. De Mey, O. Schober, M. Schäfers, C. Bremer, B. Riemann, C. Höltke, Assessment of endothelin-A receptor expression in subcutaneous and orthotopic thyroid carcinoma xenografts in vivo employing optical imaging methods, Endocrinology 153 (6) (2012) 2907–2918, https://doi.org/10.1210/en.2011-2017.
[90] N.S. Süslü, O. Katar, M. Tuncel, Role of indocyanine green combined with radiotracer-Technetium 99 m in neck surgery for primary and recurrent head and neck cancer: preliminary results of a tertiary cancer center, Eur. Arch. Oto-Rhino-Laryngol. 279 (3) (2022) 1549–1560, https://doi.org/10.1007/s00405-021-06931-1.
[91] Y. Jung, S. Kim, I. Park, J. Ryu, S.W. Kim, C.Y. Lee, J. Lee, Surgical targeting of recurrent thyroid cancer using a novel mixture of 99m-technetium macroaggregated albumin and indocyanine green, Surg. Innovat. 21 (6) (2014) 622–629, https://doi.org/10.1177/1553350614524840.
[92] W. Wei, Q. Liu, D. Jiang, H. Zhao, C.J. Kutyreff, J.W. Engle, J. Liu, W. Cai, Tissue factor-targeted ImmunoPET imaging and radioimmunotherapy of anaplastic thyroid cancer, Adv. Sci. 7 (13) (2020), 1903595, https://doi.org/10.1002/advs.201903595.
[93] S.J. Erickson-Bhatt, K.J. Mesa, M. Marjanovic, E.J. Chaney, A. Ahmad, P. Huang, Z.G. Liu, K. Cunningham, S.A. Boppart, Intraoperative optical coherence tomography of the human thyroid: feasibility for surgical assessment, Transl. Res. 195 (2018) 13–24, https://doi.org/10.1016/j.trsl.2017.12.001.
[94] L.C. Conti De Freitas, E. Phelan, L. Liu, J. Gardecki, E. Namati, W.C. Warger, G.J. Tearney, G.W. Randolph, Optical coherence tomography imaging during thyroid and parathyroid surgery: a novel system of tissue identification and differentiation to obviate tissue resection and frozen section, Head Neck 36 (9) (2013), https://doi.org/10.1002/hed.23452 n/a-n/a.
[95] R.R. Zhang, A.B. Schroeder, J.J. Grudzinski, E.L. Rosenthal, J.M. Warram, A.N. Pinchuk, K.W. Eliceiri, J.S. Kuo, J.P. Weichert, Beyond the margins: real-time detection of cancer using targeted fluorophores, Nat. Rev. Clin. Oncol. 14 (6) (2017) 347–364, https://doi.org/10.1038/nrclinonc.2016.212.
[96] P.K.C. Jonker, M.J.H. Metman, L.H.J. Sondorp, M.S. Sywak, A.J. Gill, L. Jansen, T.P. Links, P.J. van Diest, T.M. van Ginhoven, C.W.G.M. Löwik, A.H. Nguyen, R.P. Coppes, D.J. Robinson, G.M. van Dam, B.M. van Hemel, R.S.N. Fehrmann, S. Kruijff, Intraoperative MET-receptor targeted fluorescent imaging and spectroscopy for lymph node detection in papillary thyroid cancer: novel diagnostic tools for more selective central lymph node compartment dissection, Eur. J. Nucl. Med. Mol. I (2022), https://doi.org/10.1007/s00259-022-05763-3.
[97] X. Zhang, Y. Shen, J. Li, G. Chen, Clinical feasibility of imaging with indocyanine green combined with carbon nanoparticles for sentinel lymph node identification in papillary thyroid microcarcinoma, Medicine 98 (36) (2019), e16935, https://doi.org/10.1097/MD.0000000000016935.
[98] C. McMullen, D. Rocke, J. Freeman, Complications of bilateral neck dissection in thyroid cancer from a single high-volume center, JAMA Otolaryngol. Head Neck Surgery 143 (4) (2017) 376, https://doi.org/10.1001/jamaoto.2016.3670.
[99] M.S. Demarchi, B. Seeliger, J. Lifante, P.F. Alesina, F. Triponez, Fluorescence image-guided surgery for thyroid cancer: utility for preventing hypoparathyroidism, Cancers 13 (15) (2021) 3792, https://doi.org/10.3390/cancers13153792.
[100] A.V. Rudin, E. Berber, Impact of fluorescence and autofluorescence on surgical strategy in benign and malignant neck endocrine diseases, Best Pract. Res. Cl. En. 33 (4) (2019), 101311, https://doi.org/10.1016/j.beem.2019.101311.
[101] S. Sommerey, N. Al Arabi, R. Ladurner, C. Chiapponi, H. Stepp, K.K.J. Hallfeldt, J.K.S. Gallwas, Intraoperative optical coherence tomography imaging to identify parathyroid glands, Surg. Endosc. 29 (9) (2015) 2698–2704, https://doi.org/10.1007/s00464-014-3992-x.
[102] R. Ladurner, K.K.J. Hallfeldt, N. Al Arabi, H. Stepp, S. Mueller, J.K.S. Gallwas, Optical coherence tomography as a method to identify parathyroid glands, Laser Surg. Med. 45 (10) (2013) 654–659, https://doi.org/10.1002/lsm.22195.
[103] L. Pantanowitz, P. Hsiung, T.H. Ko, K. Schneider, P.R. Herz, J.G. Fujimoto, S. Raza, J.L. Connolly, High-resolution imaging of the thyroid gland using optical coherence tomography, Head Neck 26 (5) (2004) 425–434, https://doi.org/10.1002/hed.10392.
[104] J. van den Bos, L. van Kooten, S.M.E. Engelen, T. Lubbers, L.P.S. Stassen, N.D. Bouvy, Feasibility of indocyanine green fluorescence imaging for intraoperative identification of parathyroid glands during thyroid surgery, Head Neck 41 (2) (2019) 340–348, https://doi.org/10.1002/hed.25451.
[105] D.H. Kim, S.W. Kim, P. Kang, J. Choi, H.S. Lee, S.Y. Park, Y. Kim, Y. Ahn, K.D. Lee, Near-infrared autofluorescence imaging may reduce temporary hypoparathyroidism in patients undergoing total thyroidectomy and central neck dissection, Thyroid 31 (9) (2021) 1400–1408, https://doi.org/10.1089/thy.2021.0056.
[106] A. Papadia, S. Imboden, S. Mohr, S. Lanz, K. Nirgianakis, M.D. Mueller, Indocyanine green fluorescence imaging in the surgical management of an iatrogenic lymphatic fistula: description of a surgical technique, J. Minim. Invasive Gynecol. 22 (7) (2015) 1304–1306, https://doi.org/10.1016/j.jmig.2015.06.014.
[107] T. Matsutani, A. Hirakata, T. Nomura, N. Hagiwara, A. Matsuda, H. Yoshida, E. Uchida, Transabdominal approach for chylorrhea after esophagectomy by using fluorescence navigation with indocyanine green, Case Reports in Surgery 2014 (2014) 1–4, https://doi.org/10.1155/2014/464017.
[108] K. Kamiya, N. Unno, H. Konno, Intraoperative indocyanine green fluorescence lymphography, a novel imaging technique to detect a chyle fistula after an esophagectomy: report of a case, Surg. Today 39 (5) (2009) 421–424, https://doi.org/10.1007/s00595-008-3852-1.
[109] J. Chakedis, L.A. Shirley, A.M. Terando, R. Skoracki, J.E. Phay, Identification of the thoracic duct using indocyanine green during cervical lymphadenectomy, Ann. Surg Oncol. 25 (12) (2018) 3711–3717, https://doi.org/10.1245/s10434-018-6690-4.
[110] Q. Li, K. Chen, W. Huang, H. Ma, X. Zhao, J. Zhang, Y. Zhang, C. Fang, L. Nie, Minimally invasive photothermal ablation assisted by laparoscopy as an effective preoperative neoadjuvant treatment for orthotopic hepatocellular carcinoma, Cancer Lett. 496 (2021) 169–178, https://doi.org/10.1016/j.canlet.2020.09.024.
[111] H. Kobayashi, P.L. Choyke, Near-infrared photoimmunotherapy of cancer, Accounts Chem. Res. 52 (8) (2019) 2332–2339, https://doi.org/10.1021/acs.accounts.9b00273.
[112] K. Nakano, Progress of molecular targeted therapy for head and neck cancer in clinical aspects, Mol. Biomed. 2 (1) (2021) 15, https://doi.org/10.1186/s43556-021-00032-5.